ACS OMEGA

Open Access

http://pubs.acs.org/journal/acsodf

Article

Comprehensive Proteomic Profiling of Converted Adipocyte-like Cells from Normal Human Dermal Fibroblasts Using Data-Independent Acquisition Mass Spectrometry

Sunkyu Choi,* Rajaa S. D. Dalloul, Praveen Babu Vemulapalli, Sondos Yousef, Neha Goswami, and Frank Schmidt*

Cite This: *ACS Omega* 2024, 9, 40034−40050

Read Online

ACCESS | Metrics & More | Article Recommendations | Supporting Information

ABSTRACT: Adipocytes play an important role in the regulation of systemic energy homeostasis and are closely related to metabolic disorders, such as type-2 diabetes and inflammatory bowel diseases. Particularly, there is an increasing need for a human adipocyte model for studying metabolic diseases and obesity. However, utilizing human primary adipocyte culture and stem-cell-based models presents several practical limitations due to their time-consuming nature, requirement for relatively intensive labor, and high cost. Here, we applied direct conversion of normal human dermal fibroblasts (NHDFs) into adipocyte-like cells using an adipogenic cocktail containing 3-isobutyl-1-methylxanthine (IBMX), dexamethasone, insulin, and rosiglitazone and confirmed prominent lipid droplet accumulation in the converted cells. For profiling the proteome changes in the converted cells, we conducted a comprehensive quantitative proteome analysis of both the intracellular and extracellular proteome fractions using data-independent acquisition mass spectrometry. We observed that several proteins, which are known to be highly expressed in adipocytes specifically, were dominantly increased in the converted cells. In this study, we suggest that NHDFs can be converted into adipocyte-like cells by an adipogenic cocktail and can serve as a useful tool for studying human adipocytes and their metabolism.

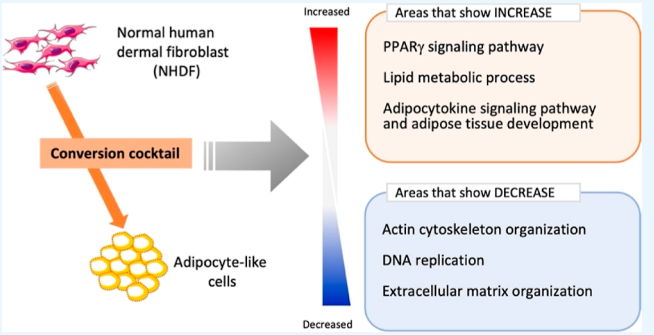

INTRODUCTION

Adipocytes are specialized cells that play a central role in energy balance and intermediary metabolism and are closely associated with metabolic disorders.[1,2] Adipocytes are not only the major energy reservoir in the body which convert excess energy sources into triglycerides but also endocrine cells that secrete various cell-to-cell signaling proteins, the so-called adipokines. For more than two decades, the understanding of adipocyte differentiation and function has been extensively studied to investigate metabolic homeostasis. A murine preadipocyte cell line, 3T3-L1, is widely used for the study of adipocytes.[3−5] Additionally, some human adipocyte cell lines have also been investigated, such as hMADS cells isolated from the stromal vascular fraction of infant adipose tissue and SGBS cells derived from a boy with the Simpson−Golabi−Behmel syndrome.[6,7] Embryonic stem cells or induced pluripotent stem cells (iPSCs) can be differentiated into adipocytes as well; however, such differentiation is time-consuming, requires relatively intense labor, and has a high cost as well. Primary adipose cells can also be used; however, given their limited lifespan and expansion capacity, it is challenging to culture and maintain them.

Recently, it has been reported that fibroblasts can be converted into various tissue cells, such as cardiomyocytes, osteoblasts, and adipocytes, by transducing transcription factors that play key roles in the differentiation into the tissue cells.[8−10] Several studies have reported that human dermal fibroblasts can be converted into adipocyte-like cells or brown adipocytes directly.[11−13] Dermal fibroblasts, which are the most abundant cells in the dermis, play a key role in the synthesis and remodeling of the extracellular matrix (ECM) and communicating with other skin cells via autocrine and paracrine interactions.[14] These studies imply that culturing dermal fibroblasts from the human dermis can be achieved through a quick and straightforward procedure to transform them into human adipocyte-like cells. This approach offers a cost-effective and convenient method to directly induce their conversion into human adipocyte-like cells for studying human adipocytes.[12,15] However, comprehensive proteome profiling of the resulting adipocyte-like cells from human dermal

Received: June 24, 2024
Revised: August 28, 2024
Accepted: September 1, 2024
Published: September 9, 2024

fibroblasts has not yet been carried out. Therefore, proteomic studies are necessary to achieve an integrated analysis of the cells' proteome. Here, we performed comprehensive quantitative proteomic analysis of extracellular proteome as well as intracellular proteome between normal human dermal fibroblasts (NHDFs) and directly converted adipocyte-like cells from NHDFs using the data-independent acquisition mass spectrometry (DIA-MS) approach. Our quantitative proteomic profiling advances our knowledge of adipocyte-like cells derived from NHDFs for studying the human adipocyte and its metabolism.

EXPERIMENTAL PROCEDURES

NHDF Cell Culture and Conversion into Adipocyte-like Cells. The NHDF cell line (Lonza, catalog no. CC-2511) was kindly donated by Dr. Nasrin Mesaeli's lab at Weill Cornell Medicine—Qatar. NHDF cells were grown in Dulbecco's modified Eagle's medium (DMEM) supplemented with 10% fetal bovine serum and 1% penicillin−streptomycin (#P0781, Sigma-Aldrich) in a humidified air at 37 °C containing 5% CO_2. At 50−60% confluency, the cells were initiated to convert into adipocyte-like cells for 2 days by adding an adipogenic cocktail containing 0.5 mM 3-isobutyl-1-methylxanthine (IBMX), 1 μM dexamethasone, 1 μM insulin, and 1 μM rosiglitazone.[12] Cells were then cultured with DMEM with insulin and rosiglitazone for 2 days. Cells were maintained in DMEM with rosiglitazone until the appearance of small lipid droplets. For extracellular proteome analysis, NHDF and adipocyte-like cells were cultured in serum-free DMEM for 24 h. Six biological replicates (interday) for quantitative analysis of intracellular proteome and extracellular proteome were prepared.

Oil Red O Staining. Cells were applied to the Oil Red O staining assay (Sigma-Aldrich, #MAK194). Briefly, cells were washed with PBS and then fixed with a 10% formalin solution for 30 min. Cells were then washed with water, and 60% isopropanol was added for 5 min. In the final step, an Oil Red O staining solution was added for 20 min and then washed with water.

Sample Preparation for Quantitative Proteome Analysis by LC−MS/MS. NHDF and adipocyte-like cells were washed with PBS three times and then harvested with LYSE buffer (PreOmics GmbH, Martinsried, Germany),[16,17] followed by sonication. Cell lysates were then centrifuged at 13,000 ×*g* at 4 °C for 15 min, and the supernatants were collected in a fresh 1.5 mL e-tube. For estimation of protein concentration, each sample was measured by a Pierce BCA Protein Quantitation Kit (Thermo Fisher Scientific). 10 μg of protein sample was digested with trypsin using the PreOmics iST kit (PreOmics GmbH, Martinsried, Germany).[16,17] Briefly, each protein sample was subjected to reduction and alkylation by LYSE buffer at 95 °C for 10 min and then to Lys-C and trypsin diegestion by DIGEST buffer at 37 °C for 3 h. After digestion, each peptide sample was quenched by STOP buffer and then loaded onto a cartridge. Each peptide sample was then washed with WASH buffer 1 and WASH buffer 2 at 3800 g for 3 min. In the final step, each peptide sample was eluted by ELUTE buffer at 3800 g for 3 min and dried using a speed vacuum chamber. Each dried peptide sample was reconstituted and sonicated in LC-LOAD buffer for LC−MS/MS analysis. For extracellular proteome analysis, the cultured media (CM) were collected and centrifuged at 3000 ×*g* at 4 °C for 15 min to eliminate all cellular debris and then filtered through a 0.20 μm filter. CM were then transferred to new tubes and concentrated to 100 μL using an Amicon Ultra-15 Centrifugal Filter unit 3 kDa molecular weight cutoff (Merck, no. UFC900324) at 4000 ×*g* at 4 °C to collect extracellular proteome.

DIA-MS Analysis. DIA-MS analysis was performed by a nanoflow chromatographic system (Vanquish Neo UHPLC system, Thermo Scientific) coupled to an Orbitrap Exploris 480 mass spectrometer (Thermo Scientific). 500 ng of peptide samples was injected by an autosampler, trapped into an Acclaim PepMap 100 Nano-Trap Column (particle size 5 μm, 100 Å, I.D.100, and length 2 cm, Thermo Scientific), and then separated with an EASY-spray PepMap Neo UHPLC C18 column (particle size 2 μm, 100 Å, I.D.75 μm, and length 50 cm, Thermo Scientific) by a 120 min gradient from buffer A (0.1% formic acid in distilled water (DW)) to buffer B (80% ACN and 0.1% formic acid). Briefly, the LC gradient was ramped from 3% buffer B to 25% buffer B in 85 min at a flow rate of 250 nL/min and then ramped to 40% buffer B in 8 min at a flow rate of 250 nL/min. For the column washing step, 100% buffer B at 250 nL/min flow was maintained for 10 min. Separated peptide samples were ionized by 2.2 kV spray voltage and then introduced into the Orbitrap Exploris 480 mass spectrometer (Thermo Scientific) by an EASY-Spray Source (Thermo Scientific) at 45 °C column temperature. Full scan mode was applied with 350−1200 m/z scan range at 120,000 orbitrap resolution, 40% RF lens, custom automatic gain control (AGC) target, 300% normalized AGC target, auto maximum injection time mode, and 1 microscans. For targeted MS/MS scan analysis, a 35 m/z isolation window, 30,000 orbitrap resolution, 40% RF lens, custom AGC target, 1000% normalized AGC target, auto maximum injection time mode, 1 microscans, and 30% higher energy collisional dissociation (HCD) collision energy were applied.

Data-Dependent Acquisition Mass Spectrometry Analysis. For data-dependent acquisition (DDA) analysis, the peptide samples were analyzed by the DDA method with a 180 min gradient from buffer A (0.1% formic acid) in DW to buffer B (80% ACN and 0.1% formic acid) in 45 °C column temperature. To increase the efficiency of peptide separation for DDA analysis, the shallow gradient was applied. Buffer B was ramped from 3 to 25% in 148 min at a flow rate of 250 nL/min and then ramped to 40% in 8 min at a flow rate of 250 nL/min. For the washing step, buffer B was ramped to 100% for 10 min. Eluted peptides were ionized and introduced into the Orbitrap Exploris 480 mass spectrometer (Thermo Scientific) by an EASY-Spray Source (Thermo Scientific) with 2.3 kV spray voltage. Full scan mode was acquired with 400−1650 m/z scan range at 120 k resolution, normalized AGC target 300%, 1 microscans, and auto maximum injection time mode. For MS/MS scan, data-dependent analysis was applied with 30 k resolution, 60 s dynamic exclusion, 2 isolation windows (m/z), custom AGC target mode, 250% normalized AGC target, auto maximum injection time mode, and 1 microscans. For fragmentation of the precursor ions, a 28% HCD collision energy was used.

Data Analysis. The DIA-MS raw data files were processed for protein identification and quantification by Spectronaut 18 software (Biognosys) with a library-free approach (direct DIA) mode using the *Homo sapiens* UniProt fasta database (release 2023_08, 82,427 protein entries) and contaminant fasta database. For modification search, carbamidomethylation (+57.021 Da) of cysteine was selected as a fixed modification,

https://doi.org/10.1021/acsomega.4c05852
ACS Omega 2024, 9, 40034−40050

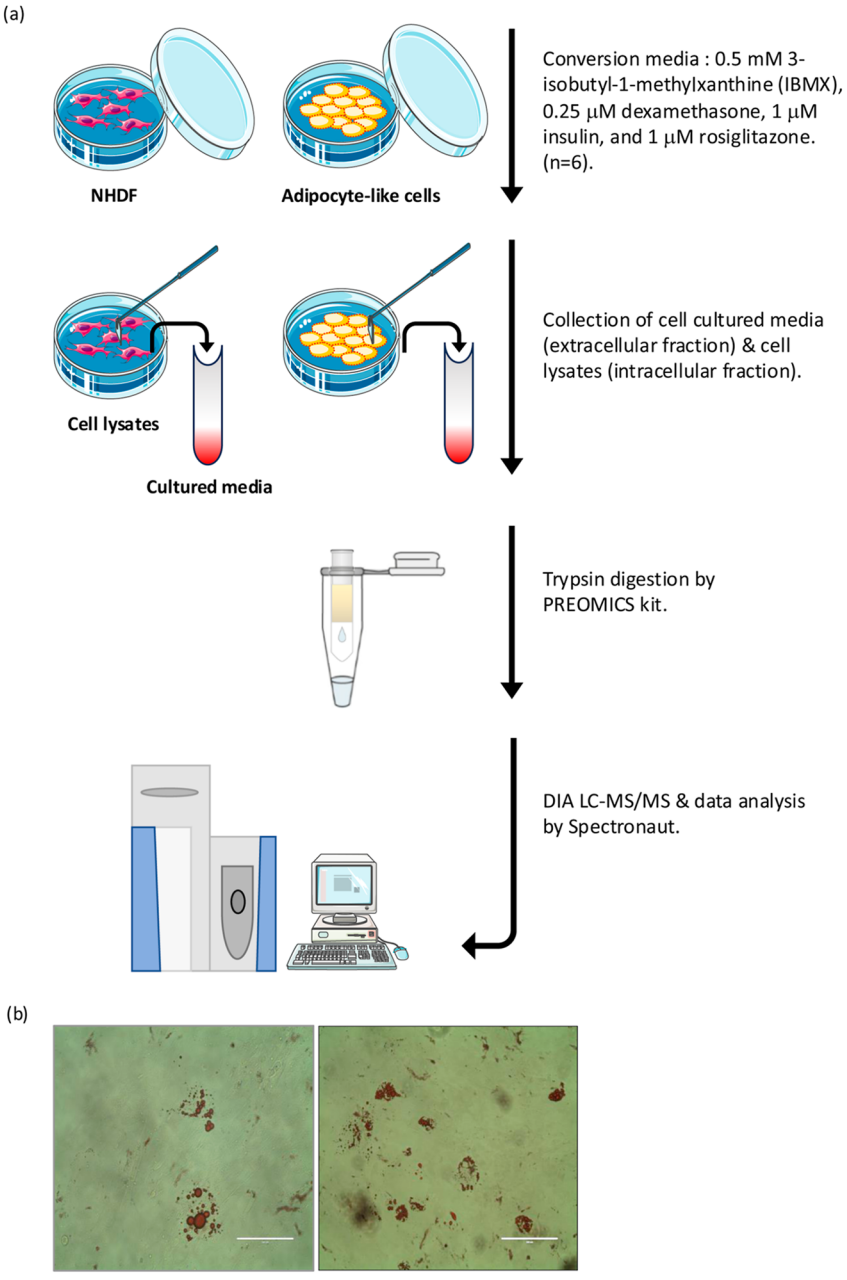

Figure 1. (a) Scheme of comprehensive proteomic profiling of converted adipocyte-like cells from NHDFs. NHDFs were cultured and converted into adipocyte-like cells by adding 0.5 mM 3-isobutyl-1-methylxanthine (IBMX), 0.25 μM dexamethasone, 1 μM insulin, and 1 μM rosiglitazone. Intracellular proteome (cell lysate fraction) and extracellular proteome (CM) were collected and analyzed by DIA-MS. The illustrations were created by adopting templates from Servier Medical Arts (https://smart.servier.com/) which is licensed under a Creative Commons Attribution 3.0 Unported License. (b) Oil Red O staining of converted adipocyte-like cells from NHDF by the adipogenic cocktail. Scale bar = 100 μm (left) and 200 μm (right).

and coupled with the N-terminal, acetylation (+42.011 Da) and oxidation (+15.995 Da) of methionine were selected as variable modifications. For other search parameters, 5−52 amino acids for the peptide length, 20 ppm tolerance for MS and MS/MS search, run-wise imputing for the imputation strategy, and sum peptide quantity for major quantity, single-hit exclusion, and Quant 2.0 (SN standard) protein LFQ method were applied. In the results, proteins that were quantified with probability value (p-value) less than 0.05 and fold ratio more than 2-fold were considered for further analysis.

For DDA analysis, the data-dependent acquisition mass spectrometry raw data files were analyzed by SpectroMine software (Biognosys) using the *H. sapiens* UniProt fasta database (release 2023_08, 82,427 protein entries) for label-free quantification. The same search parameters were applied as described in DIA-MS analysis.

The raw data generated in this study have been deposited to the ProteomeXchange Consortium (http://proteomecentral.proteomexchange.org) via the PRIDE[18] partner repository with the data set identifier PXD050528.

Bioinformatics Processing. For overall representation analysis of the changed proteins, we examined functional annotation analysis using gene ontology (GO) terms by DAVID bioinformatics resources (http://david.abcc.ncifcrf.

https://doi.org/10.1021/acsomega.4c05852
ACS Omega 2024, 9, 40034−40050

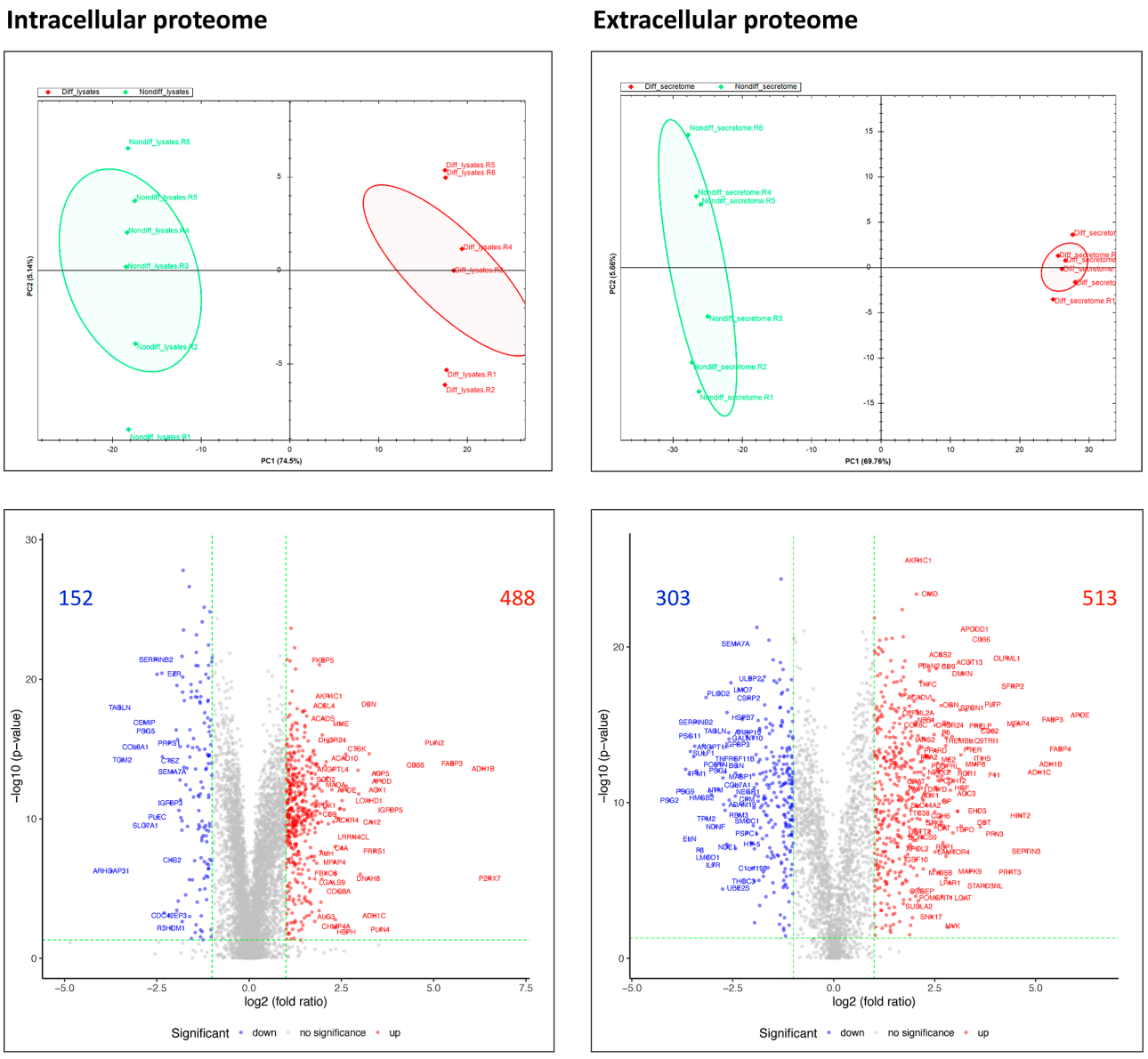

Figure 2. PCA and volcano plot distributions of the proteins in the cells. PCA distributions indicate separation between NHDF and adipocyte-like cells. Green color indicates NHDF, and red color indicates converted adipocyte-like cells. Volcano plot distributions show proteins quantified to be increased/decreased in adipocyte-like cells. Red color indicates increased proteins, and blue color indicates decreased proteins. The dotted green lines indicate that the ratio is more than 2-fold, and the significance threshold is p-value < 0.05.

gov/). To reduce redundant lists of GO terms, the open-source software REVIGO (reduce + visualize GO; http://revigo.irb.hr/) was applied.[19] The entire gene list of identified proteins was used as the background (threshold count = 3) for the calculation of over-represented GO terms, and terms with p-value < 0.05 were selected.

Analysis of Protein Expression in Adipocyte/Adipose Tissue by the Human Protein Atlas. Proteins that showed more than 2-fold increase and/or decrease in its levels in adipocyte-like cells were analyzed to compare protein expression levels against the single-cell-type RNA (adipocytes) and tissue RNA (adipose tissue) available in The Human Protein Atlas (https://www.proteinatlas.org/).

RESULTS

DIA-MS-Based Quantitative Proteome Analysis of Converted Adipocyte-like Cells. Figure 1(a) shows our strategy for quantitative analysis of intracellular proteome and extracellular proteome in the converted NHDF cells into adipocyte-like cells using DIA-MS. We directly converted NHDF cells into adipocyte-like cells using an adipogenic cocktail containing 0.5 mM 3-isobutyl-1-methylxanthine (IBMX), 1 μM dexamethasone, 1 μM insulin, and 1 μM rosiglitazone in DMEM by culturing for 28 days.[12] Intracellular lipid accumulations in adipocyte-like cells were visualized by Oil Red O staining as shown in Figure 1(b) and Supporting Information Figure 1.

In this study, 5548 proteins in the cell lysate (intracellular proteome) fraction and 2824 proteins in the CM (extracellular proteome) fraction were identified and quantified after single-hit exclusion. Among these proteins, 640 in cell lysate fraction and 816 in CM fraction exhibited more than 2-fold ratio statistically significance with p-value < 0.05 in adipocyte-like cells (Supporting Information data 1). As shown in Figure 2,

https://doi.org/10.1021/acsomega.4c05852
ACS Omega 2024, 9, 40034−40050

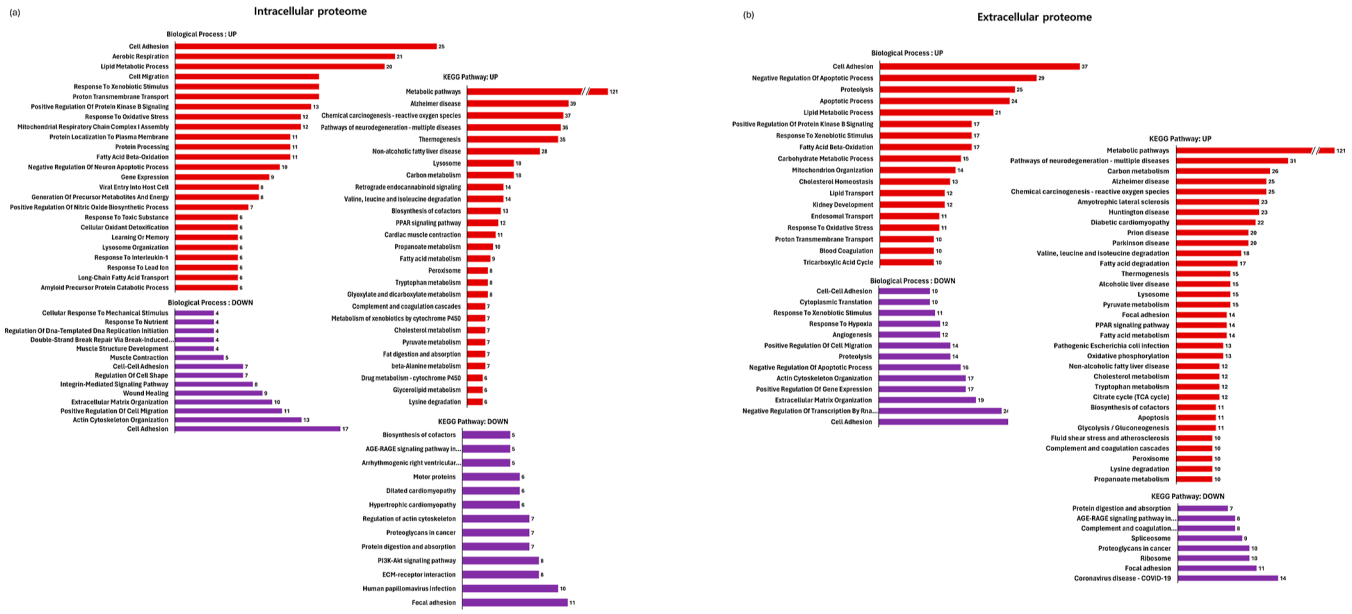

Figure 3. Functional annotations of increased/decreased proteins in adipocyte-like cells using DAVID bioinformatics resources (http://david.abcc.ncifcrf.gov/) and open-source software REVIGO (reduce + visualize GO; http://revigo.irb.hr/). (a) Biological process classification of increased/decreased (more than 2-fold) proteins and KEGG pathway analysis of increased/decreased (more than 2-fold) proteins in intracellular proteome. (b) Biological process classification of increased/decreased (more than 2-fold) proteins and KEGG pathway analysis of increased/decreased (more than 2-fold) proteins in extracellular proteome.

principal component analysis (PCA) shows clear cluster separation of the NHDF and adipocyte-like cells in the cell lysate fraction and CM fraction, respectively, and volcano plots exhibited statistically significant changes in adipocyte-like cells (with 488 proteins that showed an increase in its level and 152 proteins that exhibited a decrease in cell lysate fraction and with 513 proteins that exhibited an increase and 303 proteins that showed a decrease in CM fraction). To support DIA results in this study, DDA-based label-free quantitative analysis was also performed with the same sample set.

Quantitative Protein Changes in Converted Adipocyte-like Cells. Functional annotation analysis using GO terms and KEGG pathway analysis of increased/decreased proteins were conducted (Supporting Information data 2). Significantly enriched ($p < 0.05$) terms in the GO biological process[20] and KEGG pathway[21] analysis are shown in Figure 3a,b. Proteins that showed increased levels in this study were mainly associated with terms such as cell adhesion, aerobic respiration, and the lipid metabolic process, while proteins that exhibited decreased levels were associated with terms such as cell adhesion, actin cytoskeletal organization, positive regulation of cell migration, and DNA replication. In the KEGG pathway, metabolic pathways, Alzheimer disease, chemical carcinogenesis—reactive oxygen species, thermogenesis, and peroxisome proliferator-activated receptor γ (PPARγ) pathway exhibited increased levels, whereas focal adhesion, human papillomavirus infection, ECM—receptor interaction, and ribosome showed decreased levels.

In this study, several proteins that could be used as marker proteins of adipocyte such as fatty acid-binding protein 4 (FABP4), platelet glycoprotein 4 (CD36), long-chain fatty acid CoA ligase 1 (ACSL1), fatty acid synthase (FASN), phosphatidate phosphatase LPIN1 (LPIN1), perilipin-2 (PLIN2), perilipin-4 (PLIN4), and leptin (LEP) were observed to be predominantly increased in adipocyte-like cells[22−26] in DIA and DDA analysis, while one of the most important adipokine secreted by adipocytes, adiponectin, was identified by a single tryptic peptide, which exhibited to be increased by 2.9-fold (data not shown).

Tables 1 and 2 show the top 50 proteins that were observed as increasing or decreasing in adipocyte-like cells. Among the top 50 increased proteins, P2X purinoceptor 7 (P2Rx7) and all-trans-retinol dehydrogenase [NAD$^{(+)}$] ADH1B (ADH1B) in cell lysate fraction and apolipoprotein E (APOE) in CM fraction displayed prominently higher values in adipocyte-like cells. DDA analysis also observed ADH1B and APOE to be highly increased in adipocyte-like cells. P2Rx7 is the family of ATP-sensitive ionotropic P2X receptor that is expressed in various tissues and cell types.[27] Among the protein functions, this receptor is involved in proinflammatory cytokine processing and releasing and initiation of cell death via apoptotic and necrotic pathways.[28] It is reported that P2Rx7 is highly expressed in human adipocytes with metabolic syndrome, which might induce to the subclinical inflammation.[29] ADH1B was observed in the cell lysate fraction and CM fraction by DIA and DDA analysis. Cellular locations of ADH1B are the nucleoplasm, cytosol, and plasma membrane. However, there is no information regarding the secretion of ADH1B from adipocytes. A recent study has reported that ADH1B is highly expressed by insulin signaling in adipocytes and may play an important role in obesity and insulin resistance.[30] Another study also reports that ADH1B is involved in the differentiation of brown adipose tissue and highly expressed in brown adipoprogenitor cells.[31] APOE is a major component of lipoproteins, which is highly expressed and secreted by adipocytes, and its expression is regulated by PPARγ agonists.[32] Several studies reported that APOE promotes lipid accumulation in response to PPARγ agonists and adipocyte differentiation.[33−35]

PPARγ Signaling Pathway. Some important proteins associated with the PPARγ signaling pathway, including FABP4, FABP5, CD36, ACSL1, ACSL3, ACSL4, PLIN2,

https://doi.org/10.1021/acsomega.4c05852
ACS Omega 2024, 9, 40034−40050

Table 1. List of Top 50 Proteins Identified to be Increased in Converted Adipocyte-like Cells

increase cell lysate fraction			
gene name	**protein names**	**Log_2 ratio**	***p*-value**
P2RX7	P2X purinoceptor 7	6.52	1.89×10^{-6}
ADH1B	all-trans-retinol dehydrogenase [NAD(+)] ADH1B	6.34	2.55×10^{-14}
FABP3	fatty acid-binding protein, heart	5.50	1.09×10^{-14}
PLIN2	perilipin-2	5.02	3.61×10^{-16}
CD36	CD36 molecule (fragment)	4.50	1.43×10^{-14}
IGFBP5	insulin-like growth factor-binding protein 5	3.83	2.37×10^{-11}
APOD	apolipoprotein D (Fragment)	3.59	2.05×10^{-13}
ACP5	tartrate-resistant acid phosphatase type 5	3.56	5.81×10^{-14}
PLIN4	perilipin 4	3.55	8.55×10^{-3}
AOX1	aldehyde oxidase	3.48	8.53×10^{-13}
SCARB1	SCARB1 protein	3.43	5.51×10^{-14}
OSBP2	oxysterol-binding protein	3.43	1.82×10^{-13}
FRRS1	ferric-chelate reductase 1	3.40	2.11×10^{-8}
ADH1C	alcohol dehydrogenase 1C	3.39	8.86×10^{-4}
CA12	carbonic anhydrase 12	3.33	1.75×10^{-10}
PRXL2A	peroxiredoxin-like 2A	3.26	2.23×10^{-15}
LOXHD1	lipoxygenase homology PLAT domains 1	3.25	5.02×10^{-12}
DCN	decorin	3.24	6.16×10^{-19}
DNAH8	dynein axonemal heavy chain 8	3.23	1.91×10^{-6}
PDPN	podoplanin	3.01	9.52×10^{-7}
CD82	CD82 antigen	2.97	1.68×10^{-12}
SNCA	alpha-synuclein	2.95	3.38×10^{-14}
CTSK	cathepsin K	2.92	9.74×10^{-16}
LRRN4CL	LRRN4 C-terminal-like protein	2.83	2.01×10^{-9}
ACKR4	atypical chemokine receptor 4	2.66	1.26×10^{-10}
APOE	apolipoprotein E	2.65	9.01×10^{-13}
COL15A1	collagen type XV alpha 1 chain	2.64	4.64×10^{-13}
HEPH	hephaestin	2.63	1.28×10^{-2}
CRYL1	lambda-crystallin homologue	2.62	2.37×10^{-15}
ACAD10	acyl-CoA dehydrogenase family member 10	2.59	4.59×10^{-15}
GPNMB	glycoprotein nmb	2.57	2.21×10^{-11}
PAPOLA	poly(A) polymerase	2.52	5.05×10^{-12}
DPYD	dihydropyrimidine dehydrogenase [NADP(+)]	2.51	9.21×10^{-13}
C4A	complement C4-A	2.50	1.26×10^{-8}
MME	neprilysin	2.49	1.59×10^{-17}
PTX3	pentraxin-related protein PTX3	2.47	1.86×10^{-11}
PPL	periplakin	2.45	2.00×10^{-11}
SOD3	extracellular superoxide dismutase [Cu−Zn]	2.44	9.34×10^{-11}
COQ8A	atypical kinase COQ8A, mitochondrial	2.43	1.58×10^{-5}
ROR1	inactive tyrosine-protein kinase transmembrane receptor	2.36	8.40×10^{-11}
CHMP4A	charged multivesicular body protein 4a	2.36	5.19×10^{-3}
MAOA	amine oxidase [flavin-containing] A	2.34	3.64×10^{-13}
ARHGAP10	Rho GTPase-activating protein 10	2.34	1.72×10^{-3}
OAS3	2′-5′-oligoadenylate synthetase 3	2.34	8.34×10^{-7}
PRELP	prolargin	2.33	9.97×10^{-9}
GPR179	G protein-coupled receptor 179	2.32	6.45×10^{-3}
MFAP4	microfibril associated protein 4	2.31	1.29×10^{-7}
SLC9A9	sodium/hydrogen exchanger 9	2.29	1.65×10^{-10}
ANGPTL4	angiopoietin-related protein 4	2.27	2.86×10^{-14}
DHCR24	delta(24)-sterol reductase	2.25	2.32×10^{-16}
increase CM fraction			
gene names	**protein names**	**Log_2 ratio**	***p*-value**
APOE	apolipoprotein E	6.10	2.36×10^{-16}
FABP4	fatty acid-binding protein, adipocyte	5.61	3.55×10^{-14}
FABP3	fatty acid-binding protein, heart	5.42	4.59×10^{-16}
ADH1B	all-trans-retinol dehydrogenase [NAD(+)] ADH1B	5.37	3.39×10^{-13}
ADH1C	alcohol dehydrogenase 1C	5.09	1.12×10^{-12}
SEPTIN3	septin 3	4.77	1.34×10^{-7}
HINT2	adenosine 5′-monophosphoramidase HINT2	4.62	6.82×10^{-10}

https://doi.org/10.1021/acsomega.4c05852
ACS Omega 2024, 9, 40034−40050

Table 1. continued

increase CM fraction			
gene names	protein names	Log_2 ratio	*p*-value
MFAP4	microfibril-associated protein 4	4.57	8.31×10^{-16}
CNTN1	contactin-1	4.45	1.18×10^{-15}
SFRP2	secreted frizzled-related protein 2	4.43	3.37×10^{-18}
PRRT3	proline-rich transmembrane protein 3	4.36	2.91×10^{-6}
OLFML1	olfactomedin-like protein 1	4.29	5.32×10^{-20}
PFN3	profilin-3	3.99	1.03×10^{-8}
F11	coagulation factor XI	3.98	1.68×10^{-12}
PLTP	phospholipid transfer protein	3.94	4.90×10^{-17}
CD82	CD82 antigen	3.87	2.52×10^{-15}
STARD3NL	STARD3 N-terminal like	3.75	2.23×10^{-5}
DBT	dihydrolipoamide acetyltransferase component of pyruvate dehydrogenase complex	3.73	1.92×10^{-9}
ECH1	delta(3,5)-delta(2,4)-dienoyl-CoA isomerase, mitochondrial	3.68	1.94×10^{-15}
ITIH5	interalpha-trypsin inhibitor heavy chain 5	3.67	1.42×10^{-13}
CD36	CD36 molecule (Fragment)	3.65	3.28×10^{-21}
PRELP	prolargin	3.64	1.15×10^{-15}
MAN1C1	mannosyl-oligosaccharide 1,2-alpha-mannosidase IC	3.63	3.66×10^{-9}
EHD3	EH domain-containing protein 3	3.56	3.37×10^{-10}
APOD	apolipoprotein D (fragment)	3.52	1.16×10^{-15}
MMP8	neutrophil collagenase	3.51	3.37×10^{-13}
APCDD1	protein APCDD1	3.49	7.12×10^{-22}
PTER	phosphotriesterase-related protein	3.45	4.04×10^{-14}
SPON1	spondin-1	3.43	8.10×10^{-17}
MAPK9	stress-activated protein kinase JNK	3.38	2.59×10^{-6}
ACOT13	acyl-coenzyme A thioesterase 13	3.36	9.75×10^{-20}
LTBP4	latent transforming growth factor beta binding protein 4	3.32	3.09×10^{-14}
ROR1	inactive tyrosine-protein kinase transmembrane receptor	3.30	1.33×10^{-12}
AOC3	membrane primary amine oxidase	3.29	2.61×10^{-11}
ALDH2	aldehyde dehydrogenase, mitochondrial	3.28	1.12×10^{-16}
TSPO	translocator protein (fragment)	3.25	5.49×10^{-9}
LCAT	lecithin-cholesterol acyltransferase (fragment)	3.20	1.33×10^{-4}
DMKN	isoform 16 of dermokine	3.19	5.10×10^{-19}
HGF	hepatocyte growth factor	3.17	1.12×10^{-11}
APOB	apolipoprotein B-100	3.17	2.49×10^{-12}
MMAB	corrinoid adenosyltransferase MMAB	3.15	3.21×10^{-9}
ARMC10	armadillo repeat-containing protein 10	3.15	8.51×10^{-14}
GPX3	glutathione peroxidase 3	3.13	1.10×10^{-16}
CFD	complement factor D	3.12	7.83×10^{-13}
PCSK9	proprotein convertase subtilisin/kexin type 9	3.12	8.50×10^{-15}
ACSL4	acyl-CoA synthetase long chain family member 4	3.07	3.67×10^{-10}
HSDL2	hydroxysteroid dehydrogenase-like protein 2	3.06	3.56×10^{-10}
LAMTOR4	regulator complex protein LAMTOR4	2.97	1.48×10^{-7}
C1QBP	complement component 1 Q subcomponent-binding protein	2.95	8.74×10^{-9}
MVK	mevalonate kinase	2.95	8.37×10^{-3}
APOE	apolipoprotein E	6.10	2.36×10^{-16}

PLIN4, acyl-CoA-binding protein (DBI), sterol 26-hydroxylase, mitochondrial (CYP27A1), and angiopoietin-related protein 4 (ANGPTL4), were found in significantly increased levels in adipocyte-like cells. These proteins are important players in adipogenesis, as it targets the expression of PPARγ, a master regulator involved in the process of adipogenesis.[36] PPARγ signaling acts as a transcriptional regulator of gene expression of these proteins, all of which contain peroxisome proliferator response elements in adipocytes.[37,38] These proteins are also directly associated with the lipid metabolism in adipocytes.

Lipid Metabolic Processes. In this study, many proteins involved in fatty acid synthesis, LD accumulation, fatty acid transport, and fatty acid beta-oxidation were observed to be increased in adipocyte-like cells (Figure 4a−c).

Among the major LD structural proteins, PLIN2, PLIN3, and PLIN4 were identified. PLIN2 and PLIN4 were highly elevated by 32-fold and 11-fold in the cell lysate fraction and 4.5-fold and 2.8-fold in the CM fraction, respectively, while PLIN3 showed no significant change in both fractions. PLIN2 is expressed ubiquitously and located in LD particle surfaces and is considered a marker protein for LDs. The biological function of PLIN4 is not well understood. However, multiple studies have noted that PLIN4 is specifically expressed in adipocytes and can be found in LDs and cytosol[39] Additionally, its presence is observed during the middle to late stages of adipocyte differentiation from human mesenchymal stem cells

https://doi.org/10.1021/acsomega.4c05852
ACS Omega 2024, 9, 40034−40050

Table 2. List of Top 50 Proteins Identified to be Decreased in Converted Adipocyte-like Cells

decrease cell lysate fraction			
gene name	protein names	Log_2 ratio	*p*-value
PSG5	pregnancy-specific beta-1-glycoprotein 5	−2.80	5.10×10^{-17}
SERPINB2	plasminogen activator inhibitor 2	−2.52	4.02×10^{-22}
SYNPO2	synaptopodin-2	−2.50	4.45×10^{-21}
PLEC	isoform 4 of plectin	−2.49	7.53×10^{-11}
LMO7	LIM domain 7	−2.36	3.71×10^{-21}
DSP	desmoplakin	−2.35	3.62×10^{-15}
DYNC1I1	cytoplasmic dynein 1 intermediate chain 1	−2.30	5.65×10^{-4}
CDC42EP3	CDC42 effector protein 3 (fragment)	−2.17	8.57×10^{-4}
PRPS1	ribose-phosphate pyrophosphokinase 1	−2.17	3.79×10^{-16}
CTSZ	cathepsin X	−2.14	6.86×10^{-15}
IGFBP3	insulin-like growth factor-binding protein 3	−2.14	7.45×10^{-12}
R3HDM1	R3H domain containing 1	−2.11	6.78×10^{-3}
CKS2	cyclin-dependent kinases regulatory subunit 2	−2.09	9.20×10^{-8}
SEMA7A	semaphorin-7A	−2.08	4.28×10^{-14}
EZR	ezrin	−2.03	4.06×10^{-21}
CNN1	calponin-1	−1.98	4.40×10^{-17}
ALDH1A1	aldehyde dehydrogenase 1A1	−1.96	3.63×10^{-4}
HSPB7	isoform 2 of heat shock protein beta-7	−1.96	2.80×10^{-20}
CSRP2	cysteine and glycine rich protein 2	−1.94	2.13×10^{-16}
SLC8A1	sodium/calcium exchanger 1	−1.92	8.07×10^{-5}
MXRA5	matrix-remodeling-associated protein 5	−1.90	2.53×10^{-11}
LTBP2	latent transforming growth factor beta binding protein 2	−1.87	1.68×10^{-13}
LMO7	LIM domain 7	−1.87	6.82×10^{-16}
F3	tissue factor	−1.86	4.37×10^{-12}
FN1	fibronectin	−1.85	8.46×10^{-11}
ALCAM	CD166 antigen	−1.82	6.58×10^{-10}
FGF2	fibroblast growth factor	−1.82	2.29×10^{-22}
RAB3B	Ras-related protein Rab-3B	−1.82	1.42×10^{-10}
NTM	neurotrimin	−1.81	2.36×10^{-3}
TPM1	tropomyosin 1	−1.80	8.58×10^{-20}
TES	testin	−1.80	6.95×10^{-21}
FLNB	filamin-B	−1.79	1.58×10^{-28}
FLNC	filamin-C	−1.78	2.97×10^{-24}
COL12A1	collagen type XII alpha 1 chain	−1.77	2.05×10^{-14}
H1−5	histone H1.5	−1.76	3.46×10^{-19}
ARID1A	AT-rich interaction domain 1A (fragment)	−1.72	2.91×10^{-5}
IRAG1	inositol 1,4,5-triphosphate receptor-associated 1	−1.71	3.74×10^{-13}
NCEH1	neutral cholesterol ester hydrolase 1	−1.68	2.41×10^{-14}
FN1	isoform 1 of fibronectin	−1.67	3.53×10^{-10}
PODXL	podocalyxin	−1.66	6.25×10^{-16}
PDLIM1	PDZ and LIM domain protein 1	−1.62	2.34×10^{-27}
RFT1	protein RFT1 homologue	−1.62	2.31×10^{-6}
S100A8	protein S100-A8	−1.61	1.01×10^{-3}
TJP2	tight junction protein 2	−1.60	3.81×10^{-15}
CNN2	calponin	−1.60	4.22×10^{-17}
RRM1	ribonucleoside-diphosphate reductase large subunit	−1.59	8.29×10^{-13}
PDLIM7	PDZ and LIM domain protein 7	−1.57	2.08×10^{-19}
PLOD2	isoform 2 of procollagen-lysine,2-oxoglutarate 5-dioxygenase 2	−1.57	2.39×10^{-20}
MYO10	myosin X	−1.56	3.80×10^{-2}
TAGLN2	transgelin-2	−1.56	7.70×10^{-20}
PSG5	pregnancy specific beta-1-glycoprotein 5	−2.80	5.10×10^{-17}
decrease CM fraction			
gene names	protein names	Log_2 ratio	*p*-value
PSG2	pregnancy-specific beta-1-glycoprotein 2	−4.07	7.07×10^{-11}
POSTN	isoform 3 of periostin	−3.80	1.66×10^{-11}
PSG9	pregnancy specific beta-1-glycoprotein 9	−3.68	1.93×10^{-11}
MMP12	macrophage metalloelastase	−3.67	7.21×10^{-13}
POSTN	isoform 2 of periostin	−3.58	1.44×10^{-12}
ELN	elastin	−3.57	2.07×10^{-8}

https://doi.org/10.1021/acsomega.4c05852
ACS Omega 2024, 9, 40034−40050

Table 2. continued

decrease CM fraction			
gene names	protein names	Log_2 ratio	*p*-value
PSG11	pregnancy-specific beta-1-glycoprotein 11	−3.56	5.18×10^{-15}
STC1	stanniocalcin-1	−3.55	5.14×10^{-14}
ALCAM	CD166 antigen	−3.47	1.11×10^{-13}
PSG5	pregnancy-specific beta-1-glycoprotein 5	−3.45	2.35×10^{-14}
SERPINB2	plasminogen activator inhibitor 2	−3.42	6.84×10^{-16}
IFI30	gamma-interferon-inducible lysosomal thiol reductase	−3.40	9.06×10^{-13}
TPM1	tropomyosin 1	−3.39	1.39×10^{-12}
F3	tissue factor	−3.31	1.14×10^{-7}
HMGB2	high-mobility group protein B2	−3.27	4.83×10^{-11}
LRRC15	leucine-rich repeat-containing protein 15	−3.22	2.07×10^{-14}
SULF1	extracellular sulfatase Sulf-1	−3.22	6.58×10^{-14}
TGFBI	transforming growth factor-beta-induced protein ig-h3	−3.16	1.76×10^{-17}
TPM2	isoform 3 of tropomyosin beta chain	−3.16	1.09×10^{-9}
LMOD1	leiomodin-1	−3.12	3.31×10^{-7}
HAPLN3	hyaluronan and proteoglycan link protein 3	−3.08	1.80×10^{-11}
ANGPT1	angiopoietin-1	−3.05	2.66×10^{-14}
TGM2	protein-glutamine gamma-glutamyltransferase 2	−3.03	3.09×10^{-11}
IL7R	interleukin-7 receptor subunit alpha	−2.99	1.02×10^{-6}
TAGLN	transgelin	−2.94	2.47×10^{-15}
NDNF	protein NDNF	−2.93	3.50×10^{-9}
NTM	neurotrimin	−2.93	1.54×10^{-11}
POSTN	periostin	−2.93	3.63×10^{-13}
PSG1	isoform 4 of pregnancy-specific beta-1-glycoprotein 1	−2.86	8.55×10^{-13}
PLOD2	procollagen-lysine 5-dioxygenase	−2.86	9.79×10^{-18}
CST6	cystatin-M	−2.85	1.41×10^{-11}
SCUBE3	signal peptide, CUB, and EGF-like domain-containing protein 3	−2.84	3.08×10^{-13}
DOHH	deoxyhypusine hydroxylase	−2.77	3.74×10^{-13}
MUCL1	mucin like 1	−2.75	3.60×10^{-5}
MET	hepatocyte growth factor receptor	−2.74	2.60×10^{-12}
SERPINB7	serpin B7	−2.73	1.33×10^{-10}
PRPS1	ribose-phosphate pyrophosphokinase 1	−2.69	1.08×10^{-12}
BDNF	brain-derived neurotrophic factor	−2.69	3.15×10^{-10}
LOXL2	lysyl oxidase homologue 2	−2.67	2.66×10^{-14}
DNMT1	DNA (cytosine-5)-methyltransferase	−2.65	4.67×10^{-8}
COL8A1	collagen alpha-1(VIII) chain	−2.64	1.62×10^{-16}
NDE1	nuclear distribution protein nudE homologue 1 (fragment)	−2.64	7.09×10^{-8}
LAYN	layilin	−2.60	3.20×10^{-15}
CEMIP	cell migration-inducing and hyaluronan-binding protein	−2.59	8.25×10^{-15}
RGMB	repulsive guidance molecule BMP coreceptor b	−2.59	6.85×10^{-11}
SERPINE1	plasminogen activator inhibitor 1	−2.55	1.98×10^{-18}
MCRIP1	Mapk-regulated corepressor-interacting protein 1	−2.48	8.25×10^{-12}
PODXL	podocalyxin	−2.46	1.48×10^{-10}
TNFRSF11B	tumor necrosis factor receptor superfamily member 11B	−2.45	1.51×10^{-13}
ACAN	aggrecan	−2.44	3.78×10^{-11}
PSG2	pregnancy-specific beta-1-glycoprotein 2	−4.07	7.07×10^{-11}

along with PLIN1.[40] It is also suggested that PLIN4 plays a role in the formation of LD in human adipocytes.[40] PLIN3 is also localized in the cytosol and the LDs, and it is reported that PLIN3 contributes to the formation and stabilization of LDs similar to PLIN2. However, PLIN3 is predominantly expressed in muscle cells, neutrophils, sebocytes, and mast cells.[41−44]

Among the acyl-CoA synthetase long-chain family, ACSL1, ACSL3, and ACSL4 were observed to be increased by 2-fold, 2.4-fold, and 4-fold in adipocyte-like cells, respectively. ACSLs are importantly involved in LD biogenesis and the formation of triacylglycerols, cholesteryl esters, and neutral lipids that constitute the cargo of lipid droplets.[45−47] ACSLs convert free long-chain fatty acid into fatty acyl-CoA esters, which is highly expressed by PPARγ as part of the program of adipocyte differentiation in TAG synthesis and storage.[48] ACSL1 is found in the mitochondria, lipid droplets, and microsomes of liver, heart, white, and brown adipose tissue and skeletal muscle. ACSL3 is primarily located at the periphery of the lipid droplets. Meanwhile, ACSL4 is present in the endosome, peroxisome, plasma membrane, and secretory pathway.[46,49,50]

FABP3, FABP4, FABP5, long-chain fatty acid transport protein 3 (SLC27A3), equilibrative nucleobase transporter 1 (SLC43A3), peroxisome proliferator-activated receptor delta (PPARD), retinol binding protein 1, and cellular retinoic acid-binding protein 2 are involved proteins in fatty acid transport. In this study, all of these were observed to increase in

https://doi.org/10.1021/acsomega.4c05852
ACS Omega 2024, 9, 40034−40050

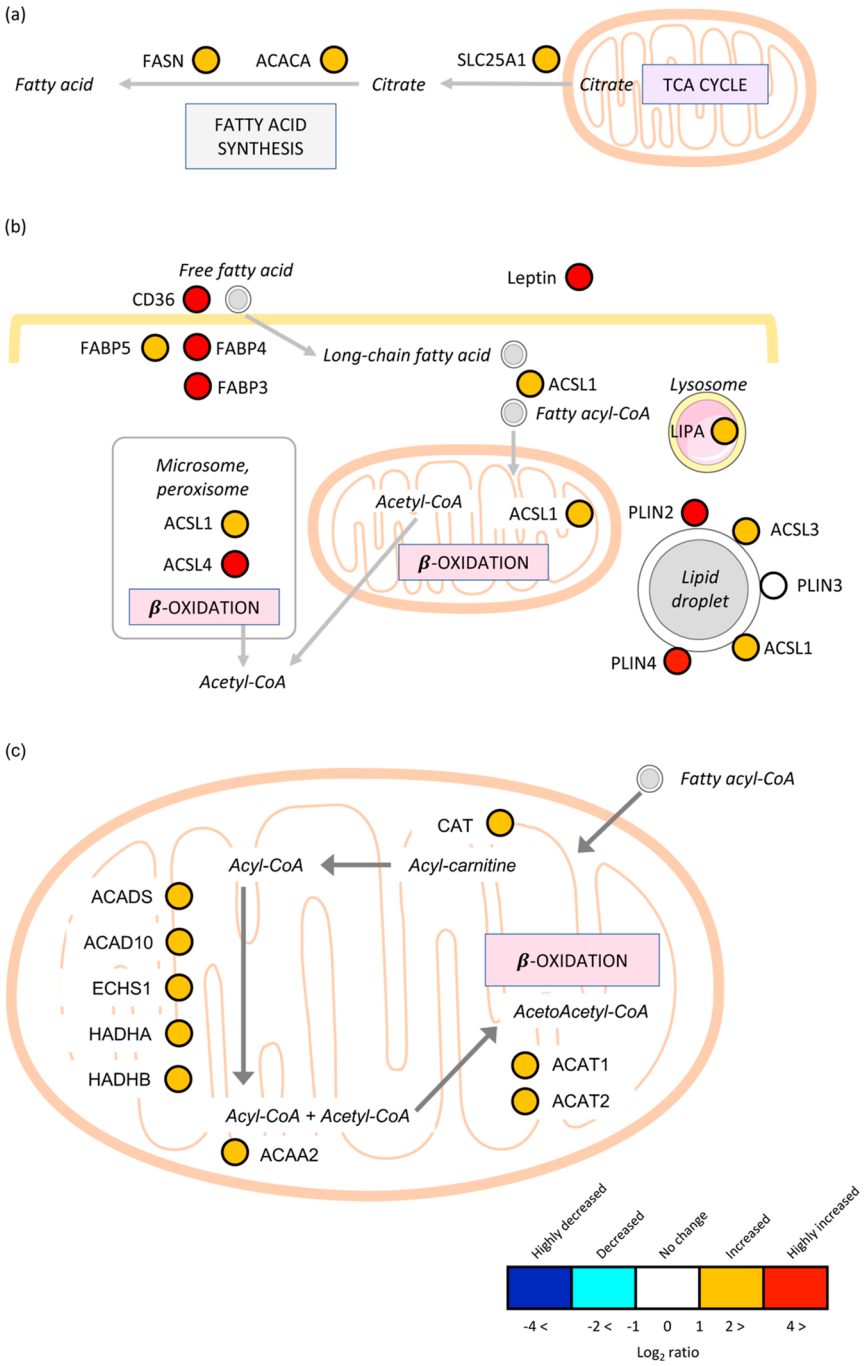

Figure 4. Increased proteins involved in (a) fatty acid synthesis and (b,c) fatty acid transport, lipid accumulation, and fatty acid beta oxidation in adipocyte-like cells. Increased/decreased fold ratio (log_2) is indicated by a color scale bar. The illustrations were created by adopting templates from Servier Medical Arts (https://smart.servier.com/) which is licensed under a Creative Commons Attribution 3.0 Unported License.

adipocyte-like cells. FABP4 exhibited to be highly increased by 42.8-fold and 48.9-fold in cell lysate fraction and CM fraction, respectively. One of the primary functions of FABPs is to serve as carriers for long-chain fatty acid carriers in blood, playing a crucial role in lipid metabolism. Specifically, FABP4, also known as an adipocyte fatty acid binding protein, is expressed and secreted by adipocytes. Interestingly, FABP3 also displayed highly elevated levels of 45.3-fold. It has been reported that the expression level of FABP3 significantly increases during acute cold exposure in brown adipocytes, whereas its expression level remains low in white adipocytes.[51−53] The level of FABP5 was shown to be increased by 2.2-fold in both fractions. It is reported that FABP5 might be secreted from adipocytes, although it remains to be elucidated. SLC27A3 and SCL43A3 were increased by 2.5-fold and 2-fold, respectively. The lipid-activated transcription factor PPARD exhibited a 5.7-fold increase in levels of adipocyte-like cells. PPARD is activated by long-chain fatty acids and mediates adipogenic action of the long-chain fatty acids by stimulating preadipocyte proliferation.[54]

A number of proteins related to fatty acid β-oxidation were observed to be elevated in adipocyte-like cells. Acyl-CoA dehydrogenases, short-chain-specific acyl-CoA dehydrogenase, mitochondrial (ACADS), and acyl-CoA dehydrogenase family

https://doi.org/10.1021/acsomega.4c05852
ACS Omega 2024, 9, 40034−40050

member 10 (ACAD10) were increased by 4-fold and 6-fold. Trifunctional enzyme subunit alpha (HADHA) and trifunctional enzyme subunit beta (HADHB) were also increased by 2-fold in the cell lysate fraction and 4.4-fold and 3.8-fold in the CM fraction, respectively. HADHA is associated with dehydrogenating the hydroxyl group to the keto group, and HADHB is an enzyme that catalyzes the thiolysis of β-ketoacyl-CoA esters as part of the fatty acid β-oxidation process. Acetyl-CoA acetyltransferase 1 and 2 (ACAT1 and ACAT2) enzymes catalyze the reversible formation of acetyl-CoA to acetoacetyl-CoA[55] and were found to be increased by 2.3-fold and 2-fold in cell lysate fraction and 4.6-fold and 3.3-fold in CM fraction, respectively. The protein in relation to the last step of the fatty acid β-oxidation pathway, 3-ketoacyl-CoA thiolase (ACAA2), was elevated by 3.2-fold. Lysosomal cobalamin transporter (ABCD4), which is known to be involved in the transport of vitamin B_{12} to the cytosol from the lysosomal lumen,[56] and lysosomal cobalamin transport escort protein (LMBD1) were increased by 3.4-fold and 2.4-fold, respectively. Other proteins related to fatty acid β-oxidation, including catalase (CAT), methylglutaconyl-CoA hydratase, mitochondrial (AUH), enoyl-CoA hydratase, mitochondrial (ECHS1), enoyl-CoA delta isomerase 1, mitochondrial (ECI1), hydroxysteroid 17-beta dehydrogenase 10 (HSD18B10), leptin (LEP), ethylmalonyl-CoA decarboxylase 1 (ECHDC1), hydroxyacyl-CoA dehydrogenase (HADH), carnitine *O*-acetyltransferase (CRAT), and 2,4-dienoyl-CoA reductase [(3E)-enoyl-CoA-producing], mitochondrial (DECR1), and dehydrogenase/reductase SDR family member 6 (BDH2) were also increased.

Adipocytokine Signaling Pathway and Adipose Tissue Development. In the CM fraction, some of the proteins involved in the adipocytokine signaling pathway and adipose tissue development were identified to be elevated in adipocyte-like cells. In particular, one of the important hormones secreted mainly by white adipose tissue, leptin, exhibited an increased level by 4.8-fold (DDA analysis also showed an increased level exhibiting a fold change of 7.4). Leptin also regulates the appetite and energy consumption. Lysosomal acid lipase/cholesteryl ester hydrolase (LIPA), which hydrolyzes cholesteryl ester and triglycerides in lipoprotein taken up by receptor-mediated endocytosis to generate free fatty acids and cholesterol, also showed an increased level by 3.7-fold. LIPA expression is modulated by transcription factor forkhead homeobox-type protein O1 (FoxO1) in adipocytes.[57] A transcriptional factor that is responsible for triggering the immune response, nuclear factor kappa B (NFKB1), is observed to be increased by 2.1-fold. It is known that the NFKB1 pathway plays a role in reprogramming the fat cell transcriptome and expression of chemokines and cytokines in adipocytes as well as immune response.[58]

Among the top 50 decreased proteins, Rho GTPase-activating protein 31 (ARHGAP31) and transgelin (TAGLN) in cell lysate fraction and pregnancy-specific beta-1-glycoprotein 2 and 9 (PSG2 and PSG9) and macrophage metalloelastase (MMP12) in CM fraction were observed to be highly decreased. ARHGAP31 is a family of Rho GTPases which regulate a variety of cellular processes by an inactive form bound to GDP and an active form bound to GTP. ARHGAP31 inactivates GTPases known as CDC42/RAC1, which play important roles in cell division, survival and migration, and the maintenance of the actin cytoskeletal structures.[59] TAGLN is an actin-cross-linking protein that belongs to the calponin family.[60] It is reported that TAGNL regulates osteoblastic and adipogenic differentiation through actin cytoskeleton organization and is identified as a potentially novel gene involved in the endocytic uptake of low-density lipoprotein.[61,62] PSGs are highly expressed by placental syncytiotrophoblast and released into the maternal circulation during pregnancy.[63,64] These proteins play a key role in regulating innate and adaptive immunity by modulating macrophage.[65] Many MMPs are expressed by mature adipocytes and by the surrounding stromal cells and known to play key critical roles in the promotion of adipose tissue expansion.[66,67] MMP12 is predominantly expressed and secreted by macrophages and trophoblasts, which regulates adipose tissue expansion and inhibits angiogenesis and suppresses vascularization.[68] In the CM fraction, one of the acute phase responsible proteins, interleukin-6 (IL6), which is a pleiotropic proinflammatory cytokine that plays a role in hematopoiesis, was observed to be decreased in adipocyte-like cells.

Actin Cytoskeleton Organization. Among the decreased protein groups, many proteins involved in actin cytoskeletal organization were observed in this study (Figure 5a). PDZ and LIM domain (PDLIM) proteins PDLIM1, PDLIM4, PDLIM5, and PDLIM7 were decreased more than 2-fold in adipocyte-like cells (Figure 5a). PDLIMs are signaling adaptors that interact with the main actin cross-linking protein, alpha-actinin, via their PDZ domains or internal regions between PDA and LIM domains.[69] The LIM domain acts on a wide range of phenomena from gene expression for the cytoskeletal remodeling.[70] It is reported that PDLIM1 binds to alpha-actinin-4 (ACTN4) competitively that prevents integrin binding and F-actin overgrowth.[71] Cysteine and glycine-rich proteins (CSRP), CSRP1 and CSRP2, were also decreased. CSPRs, which belong to the LIM domain superfamily, are localized in the nucleus and cytoplasm and preferentially expressed in muscle cells.[72] It is reported that CRPS1 regulates dynamic cell movement, and CRPS2 promotes breast cancer invasion and metastasis.[73,74] A family of the ezrin/radixin/moesin (ERM), ezrin (EZR), is highly decreased in adipocyte-like cells. EZR plays a key role as a linker between plasma membrane and actin cytoskeleton and a key role in cell surface structure adhesion, migration, and organization. Formin-like protein 3 (FMNL3), which plays a role in the reorganization of microtubules during angiogenesis, showed a decreased level. ACTN4, filamin-B and -C (FLNB and FLNC), paladin (PALLD), and hemicentin-1 (HMCN1) were observed to be decreased in adipocyte-like cells.

DNA Replication. DNA replication and cell-cycle-related proteins were decreased in adipocyte-like cells (Figure 5b). DNA replication licensing factors MCM3, MCM4, MCM5, and MCM6 and ribonucleoside-diphosphate reductase large subunit (RRM1) were observed to be decreased more than 2-fold and proliferating cell nuclear antigen were decreased by 1.5-fold. MCM proteins, which are marker proteins for cell proliferation, act as key players in DNA replication in the G1-S phase of cell cycle.

ECM Organization. Some of the proteins related to ECM organization were observed to be decreased in the CM fraction (Figure 5c). ECM is a key regulator of dermal fibroblast proliferation and migration in skin development, homeostasis, and would healing.[75] Among the collagen proteins, collagen alpha-1(I) chain (COL1A1), collagen alpha-1(V) chain (COL5A1), collagen alpha-1(VII) chain (COL7A1), collagen alpha-1(VIII) chain (COL8A1), and collagen type XII alpha 1

https://doi.org/10.1021/acsomega.4c05852
ACS Omega 2024, 9, 40034−40050

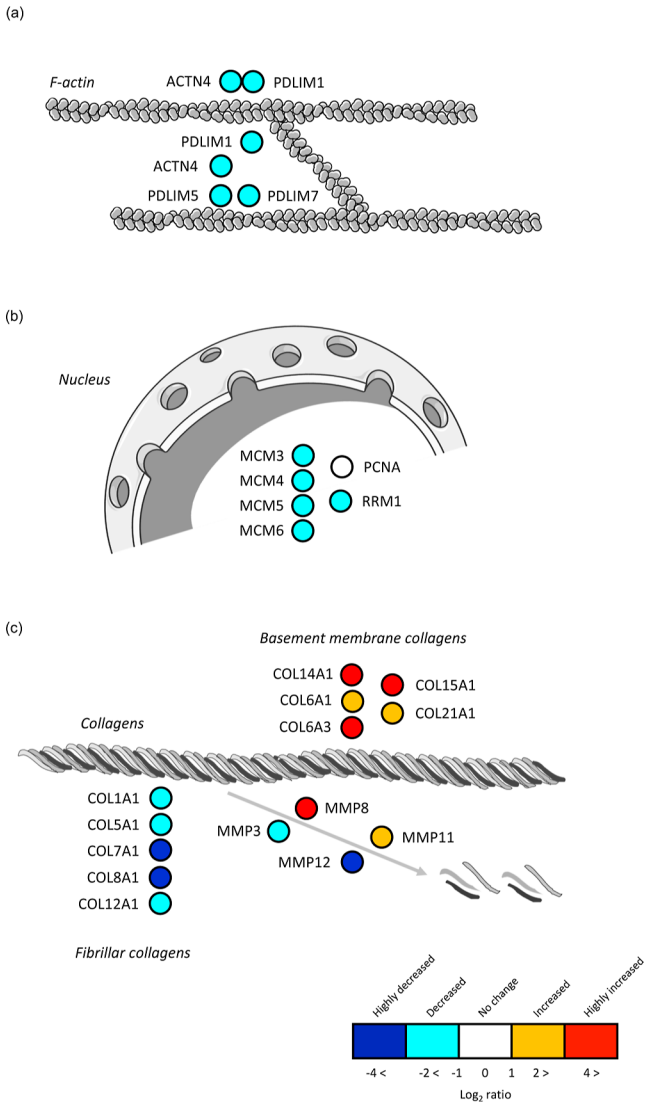

Figure 5. Decreased proteins involved in (a) cytoskeletal organization, (b) DNA replication, and (c) collagens in adipocyte-like cells. Increased/decreased fold ratio (log_2) is indicated by a color scale bar. The illustrations were created by adopting templates from Servier Medical Arts (https://smart.servier.com/) which is licensed under a Creative Commons Attribution 3.0 Unported License.

chain (COL12A1) were decreased, while collagen alpha-3(VI) chain (COL6A3), collagen alpha-1(VI) chain (COL6A1), collagen alpha-1(XIV) chain (COL14A1), collagen alpha-1(XV) chain (COL15A1), and collagen type XXI alpha 1 chain (COL21A1) were found to be increased in adipocyte-like cells. It is known that key collagens associated with white adipocytes differentiation are basement membrane collagens, such as COL4, COL6, COL15 and COL18, while undifferentiated fibroblast-related collagens are COL1, COL3, and COL5.[76] Among the matrix metalloproteinases, stromelysin-1 (MMP3) and MMP12 were observed to be decreased, while neutrophil collagenase (MMP8) and stromelysin-3 (MMP11) were increased. Many integrin subunit proteins were identified in this study. Integrin alpha-1 (ITGA1) and integrin alpha-11 (ITGA11) were observed to decrease, while integrin subunit alpha V (ITGAV) was found to be increased.

Human Protein Atlas Search. Further analysis of the proteins showing increased or decreased levels in adipocyte-like cells was conducted by using the Human Protein Atlas database search. Highly increased proteins such as marker proteins of adipocyte, FABP4, CD36, ACSL1, PLIN2, PLIN4, and LEP have shown high levels of expression in human adipocytes or adipose tissue. Decorin (DCN), alcohol dehydrogenase 1B (class I), beta polypeptide (ADH1B), and complement factor D have also shown high levels in the Human Protein Atlas database (Supporting Information data 3).

DISCUSSION

Primary adipocytes or adipose tissues are obtained by tissue biopsy and can only be studied for a short period in culture. Bone marrow mesenchymal stromal cells or primary preadipocytes can also be differentiated into adipocytes but often show low differentiation efficiency and limited proliferative and differentiation capacity.[77] Generation of adipocytes by differentiation of pluripotent human embryonic stem cells and iPSCs were also attempted by using conditional overexpression of PPARγ that showed white adipocyte characteristics even after turning off PPARγ transgene expression.[78,79] These cells also exhibited glucose uptake by insulin stimulation and inducible lipolysis, among other characteristics of adipocytes. Nevertheless, the protocol entails significant costs and labor. A recent study found that by using lentivirus to conditionally overexpress PPARγ and combining it with an adipogenic cocktail, dermal fibroblasts were efficiently converted into lipid-laden adipocyte-like cells in a simple manner.[12] Dermal fibroblasts are the most abundant cells in the dermis and can be isolated from skin biopsies.

In this study, we applied the reprograming protocol to convert NHDF into adipocyte-like cells by stimulating the cells with the adipogenic cocktail, which contains IBMX, dexamethasone, insulin, and rosiglitazone. After confirmation of prominent LD accumulation in the cells, comprehensive proteome analysis was performed by using DIA-MS analysis. Among the statistically quantified proteins, predominantly increased proteins are linked with the PPARγ signaling pathway, lipid metabolism, adipocytokine signaling pathway, and adipose tissue development, while decreased proteins are mostly involved in actin cytoskeleton organization and ECM organization. These results are consistent with our previous study that analyzed proteome changes between 3T3-L1 preadipocytes and adipocytes.[80]

The PPARγ signaling pathway has been known to play a major role in adipogenesis, which induces the expression of adipocyte-specific genes, such as adiponectin, FABP4, CD36, and PLINs. These molecules are primarily associated with regulating the termination of the adipocyte differentiation process via interaction with CCAAT/enhancer binding protein alpha (C/EBPα).[4,81,82] In this study, FABP4, CD35, and PLINs were significantly elevated, and a major hormone primarily produced by the adipocytes, leptin, was also observed to be highly increased in the converted cells. These results are indicative that NHDFs were converted into adipocyte-like cells. Several key players in the lipid metabolism and accumulation were also found to be increased by more than 2-fold, while enzymes associated with the glycolysis and citrate cycle (TCA cycle) were not found to be significantly affected in the cells. The process of fatty acid synthesis begins with the transportation of citrate by the mitochondrial citrate carrier, known as the tricarboxylate transport protein (SLC25A1). Subsequently, fatty acids are synthesized by the enzyme FASN.

https://doi.org/10.1021/acsomega.4c05852
ACS Omega 2024, 9, 40034−40050

Elevation of SLC25A1 (2.8-fold) and FASN (2.1-fold) is suggestive of an increase in citrate flux during fatty acid synthesis and lipogenesis. Acetyl-CoA carboxylase 1 (ACACA), which catalyzes carboxylation of acetyl-CoA to malonyl-CoA in the first step of fatty acid synthesis, was increased by 1.9-fold. However, other key proteins involved in fatty acid synthesis, including ATP-citrate synthase (ACLy) and stearoyl-CoA desaturase, did not show significant changes. Further in-depth study is needed to investigate fatty acid synthesis in the cells. The increase in the number of key proteins associated with fatty acid β-oxidation metabolism in this study suggests proper adipocyte function. During lipolysis, free fatty acids are transported into the mitochondria through the interaction of CD36 and FABP4. Within the mitochondria, these fatty acids are converted into acetyl-CoA via fatty acid β-oxidation metabolism and acyl-CoA synthesis before reentering the TCA cycle. It is well established that fatty acid β-oxidation in white adipocytes is therapeutically crucial as elevated free fatty acid levels affect adipocyte stress and inflammation, ultimately inducing a decrease in insulin sensitivity.[83,84]

In this study, APOE was observed to be most highly increased by 68-fold in the CM fraction in adipocyte-like cells. APOE, which is synthesized by adipocytes and is a major component of very low-density lipoproteins, is essential for adipogenesis.[35] It has also been reported that APOE initiates lipid accumulation and differentiation in human adipocytes.[34] These results suggest that a high expression level of APOE may be an indicator of adipogenesis.

The protein showing the greatest increase in the cell lysate fraction is P2Rx7, with a 91-fold upregulation. (P2Rx4 was also increased by 3.7-fold.) Several studies reported that P2Rx7 is associated with lipid metabolism, which plays an extensive role in controlling lipid storage and 3T3-L1 adipogenesis.[85−87] It is also known that suppression of CD36 downregulates differentiation of 3T3-L1 preadipocytes via the P2Rx7 pathway.[88] Therefore, we hypothesize that P2Rx7 might be significantly associated with the conversion of NHDF to adipocyte-like cells in this study.

Interestingly, ADH1B showed a significant increase of 81-fold in the cell lysate fraction and 41-fold in the CM fraction of adipocyte-like cells. It has been reported that the expression level of ADH1B in mature adipocytes from lean donors is higher compared with obese donors. Furthermore, its expression level is significantly upregulated during adipogenesis and in subcutaneous adipose tissue. Additionally, ADH1B downregulates the expression of FABP4 during adipogenesis.[30] However, despite the high expression level of ADH1B in adipocytes, its exact functional role is unknown. We assume that a high expression level of ADH1B may affect the adipocyte metabolism by downregulation of FABP4. Further investigation to elucidate the role of ADH1B in adipocytes is required.

During adipogenesis, changes in cell morphology are dramatic. Microtubules are fragmented, and actin microfilaments are extensively depolymerized. In this study, many cytoskeletal proteins were observed to decrease more than 2-fold in adipocyte-like cells. This is consistent with previous studies that show a decreased expression level of cytoskeletal proteins during adipocyte differentiation.[80,89] For adipocyte differentiation, remodeling of the ECM constitutes an important process. We also observed that fibrillar collagens, which are generally expressed in undifferentiated fibroblasts, were decreased, and basement membrane-type collagens, which are expressed in adipocytes, were increased in adipocyte-like cells.[76] These results are indicative that the collagenous matrix surrounding the cells is modified after conversion to adipocyte-like cells. After initiation of differentiation into adipocytes, the cells progress through at least two cell-cycle divisions and then express adipogenic factors such as PPARγ and C/EBPα. Following this, the cell cycle and cell proliferation are reduced in the cells. Our previous study also observed decreased proteins involved in the cell cycle progression in 3T3-L1 adipocytes.[80] Therefore, our observation of the decreasing proteins involved in DNA replication in this study is supportive of the fact that NHDF is converted into adipocyte-like cells.

Taking everything into account, these results support the direct conversion of adipocyte-like cells from NHDF using an adipogenic cocktail. Specifically, we presume that NHDFs were transformed into white adipocyte-like cells in this study, as evidenced by the significant increase in white adipocyte marker proteins such as FABP4 and leptin, while markers for brown or beige adipocytes were not detected. However, several important points still need to be elucidated. In this study, most dominantly increased proteins are CD36, FABP4, and leptin, which are known to be highly expressed in white adipocytes specifically, whereas only a single tryptic peptide of adiponectin was identified in this study. Adiponectin is also secreted exclusively by white adipocytes. It is known that the adiponectin/leptin ratio is negatively correlated by adipose tissue dysfunction.[90] Low adiponectin expression occurs in obesity, insulin resistance, and type-2 diabetes, while leptin is overexpressed in obesity. All things considered, further in-depth study for the investigation of characterization of the converted adipocyte-like cells from NHDFs is needed. It has also been reported that adipocyte-like cells reprogrammed from fibroblasts is reversible after PPARγ expression is turned off, leading to rapid delipidation.[12] This requires further investigation of reversible conversion in the cells. Despite the need for further investigations, we propose that adipocyte-like cells converted from NHDF using an adipogenic cocktail could serve as a valuable model for studying human adipocytes. This approach offers the advantages of lower cost and reduced labor.

In conclusion, we applied a protocol involving an adipogenic cocktail to convert NHDF into adipocyte-like cells and performed comprehensive proteome analysis of cell lysate fractions and CM fractions of the cells. Our previous study, along with others, has reported that PPARγ signaling and fatty acid β-oxidation metabolism are upregulated, and cell cycle and cytoskeletal proteins are downregulated during adipocyte differentiation. Our proteomic observations confirm the previous findings and provide support for the notion that NHDF were converted into adipocyte-like cells by use of an adipogenic cocktail. We hope that further functional studies based on our results provide advanced clues regarding adipogenesis and its role in related obesity and metabolic syndrome. Here, we suggest that the converted adipocyte-like cells from NHDFs using the simple protocol are helpful for the study of human adipocytes.

■ ASSOCIATED CONTENT

Supporting Information

The Supporting Information is available free of charge at https://pubs.acs.org/doi/10.1021/acsomega.4c05852.

https://doi.org/10.1021/acsomega.4c05852
ACS Omega 2024, 9, 40034−40050

Quantified proteins of DIA-MS quantitative proteomics of adipocyte-like cells; enriched biological process/KEGG pathway of increased and decreased proteins in adipocyte-like cells; and Human Protein Atlas search (XLSX)

Converted adipocyte-like cells from NHDFs by the adipogenic cocktail (PDF)

AUTHOR INFORMATION

Corresponding Authors

Sunkyu Choi − *Proteomics Core, Research, Weill Cornell Medicine-Qatar, P.O. 24144 Doha, Qatar;* orcid.org/0000-0001-8726-732X; Email: szc2010@qatar-med.cornell.edu

Frank Schmidt − *Proteomics Core, Research, Weill Cornell Medicine-Qatar, P.O. 24144 Doha, Qatar*; Email: frs4001@qatar-med.cornell.edu

Authors

Rajaa S. D. Dalloul − *Proteomics Core, Research, Weill Cornell Medicine-Qatar, P.O. 24144 Doha, Qatar*

Praveen Babu Vemulapalli − *Proteomics Core, Research, Weill Cornell Medicine-Qatar, P.O. 24144 Doha, Qatar;* orcid.org/0000-0001-8944-1731

Sondos Yousef − *Proteomics Core, Research, Weill Cornell Medicine-Qatar, P.O. 24144 Doha, Qatar*

Neha Goswami − *Proteomics Core, Research, Weill Cornell Medicine-Qatar, P.O. 24144 Doha, Qatar*

Complete contact information is available at: https://pubs.acs.org/10.1021/acsomega.4c05852

Author Contributions

S.C. designed and carried out the study. S.C., R.D., and P.V. prepared the samples for proteomics and conducted the analysis by mass spectrometry. S.C. analyzed the proteomic data and performed bioinformatics analysis. S.C. and F.S. discussed the results. N.G. provided technical and infrastructural support. S.C. drafted the manuscript with help from F.S. and N.G.

Notes

The authors declare no competing financial interest.

ACKNOWLEDGMENTS

This publication was made possible by the NPRP-Standard (NPRP-S) Twelfth (12th) Cycle grant [NPRP12S-0318-190392] from the Qatar National Research Fund (a member of Qatar Foundation). The findings herein reflect the work and are solely the responsibility of the authors. We thank Hidenori Miyagawa for edition of figures.

REFERENCES

(1) Fruhbeck, G.; Gomez-Ambrosi, J.; Muruzabal, F. J.; Burrell, M. A. The adipocyte: a model for integration of endocrine and metabolic signaling in energy metabolism regulation. *Am. J. Physiol.: Endocrinol. Metab.* **2001**, *280* (6), E827−E847.

(2) Rosen, E. D.; Spiegelman, B. M. Adipocytes as regulators of energy balance and glucose homeostasis. *Nature* **2006**, *444* (7121), 847−853.

(3) Green, H.; Meuth, M. An established pre-adipose cell line and its differentiation in culture. *Cell* **1974**, *3* (2), 127−133.

(4) Rosen, E. D.; MacDougald, O. A. Adipocyte differentiation from the inside out. *Nat. Rev. Mol. Cell Biol.* **2006**, *7* (12), 885−896.

(5) Poulos, S. P.; Dodson, M. V.; Hausman, G. J. Cell line models for differentiation: preadipocytes and adipocytes. *Exp Biol. Med.* **2010**, *235* (10), 1185−1193.

(6) Rodriguez, A. M.; Elabd, C.; Delteil, F.; Astier, J.; Vernochet, C.; Saint-Marc, P.; Guesnet, J.; Guezennec, A.; Amri, E. Z.; Dani, C.; Ailhaud, G. Adipocyte differentiation of multipotent cells established from human adipose tissue. *Biochem. Biophys. Res. Commun.* **2004**, *315* (2), 255−263.

(7) Fischer-Posovszky, P.; Newell, F. S.; Wabitsch, M.; Tornqvist, H. E. Human SGBS cells - a unique tool for studies of human fat cell biology. *Obes. Facts* **2008**, *1* (4), 184−189.

(8) Inoue, Y.; Kishida, T.; Kotani, S. I.; Akiyoshi, M.; Taga, H.; Seki, M.; Ukimura, O.; Mazda, O. Direct conversion of fibroblasts into urothelial cells that may be recruited to regenerating mucosa of injured urinary bladder. *Sci. Rep.* **2019**, *9* (1), 13850.

(9) Wakao, J.; Kishida, T.; Fumino, S.; Kimura, K.; Yamamoto, K.; Kotani, S. I.; Mizushima, K.; Naito, Y.; Yoshikawa, T.; Tajiri, T.; Mazda, O. Efficient direct conversion of human fibroblasts into myogenic lineage induced by co-transduction with MYCL and MYOD1. *Biochem. Biophys. Res. Commun.* **2017**, *488* (2), 368−373.

(10) Kishida, T.; Ejima, A.; Yamamoto, K.; Tanaka, S.; Yamamoto, T.; Mazda, O. Reprogrammed Functional Brown Adipocytes Ameliorate Insulin Resistance and Dyslipidemia in Diet-Induced Obesity and Type 2 Diabetes. *Stem Cell Rep.* **2015**, *5* (4), 569−581.

(11) Takeda, Y.; Harada, Y.; Yoshikawa, T.; Dai, P. Direct conversion of human fibroblasts to brown adipocytes by small chemical compounds. *Sci. Rep.* **2017**, *7* (1), 4304.

(12) Chen, J.-H.; Goh, K. J.; Rocha, N.; Groeneveld, M. P.; Minic, M.; Barrett, T. G.; Savage, D.; Semple, R. K. Evaluation of human dermal fibroblasts directly reprogrammed to adipocyte-like cells as a metabolic disease model. *Dis. Models Mech.* **2017**, *10* (12), 1411−1420.

(13) Sowa, Y.; Kishida, T.; Louis, F.; Sawai, S.; Seki, M.; Numajiri, T.; Takahashi, K.; Mazda, O. Direct Conversion of Human Fibroblasts into Adipocytes Using a Novel Small Molecular Compound: Implications for Regenerative Therapy for Adipose Tissue Defects. *Cells* **2021**, *10* (3), 605.

(14) Zhang, Z.; Kruglikov, I.; Zhao, S.; Zi, Z.; Gliniak, C. M.; Li, N.; Wang, M. Y.; Zhu, Q.; Kusminski, C. M.; Scherer, P. E. Dermal adipocytes contribute to the metabolic regulation of dermal fibroblasts. *Exp. Dermatol.* **2021**, *30* (1), 102−111.

(15) Feisst, V.; Brooks, A. E.; Chen, C. J.; Dunbar, P. R. Characterization of mesenchymal progenitor cell populations directly derived from human dermis. *Stem Cells Dev.* **2014**, *23* (6), 631−642.

(16) Kulak, N. A.; Pichler, G.; Paron, I.; Nagaraj, N.; Mann, M. Minimal, encapsulated proteomic-sample processing applied to copy-number estimation in eukaryotic cells. *Nat. Methods* **2014**, *11* (3), 319−324.

(17) Niu, L.; Mann, M. Quick and clean: Cracking sentences encoded in E. coli by LC-MS/MS, de novo sequencing, and dictionary search. *EuPa Open Proteomics* **2019**, *22*−*23*, 30−35.

(18) Vizcaino, J. A.; Csordas, A.; del-Toro, N.; Dianes, J. A.; Griss, J.; Lavidas, I.; Mayer, G.; Perez-Riverol, Y.; Reisinger, F.; Ternent, T.; Xu, Q. W.; Wang, R.; Hermjakob, H. 2016 update of the PRIDE database and its related tools. *Nucleic Acids Res.* **2016**, *44* (D1), D447−D456.

(19) Supek, F.; Bosnjak, M.; Skunca, N.; Smuc, T. REVIGO summarizes and visualizes long lists of gene ontology terms. *PLoS One* **2011**, *6* (7), No. e21800.

(20) The Gene Ontology Consortium. The Gene Ontology project in 2008. *Nucleic Acids Res.* **2008**, *36* (suppl_1), D440−D444.

(21) Kanehisa, M.; Goto, S. KEGG: kyoto encyclopedia of genes and genomes. *Nucleic Acids Res.* **2000**, *28* (1), 27−30.

(22) Marr, E.; Tardie, M.; Carty, M.; Brown Phillips, T.; Wang, I. K.; Soeller, W.; Qiu, X.; Karam, G. Expression, purification, crystallization and structure of human adipocyte lipid-binding protein (aP2). *Acta Crystallogr., Sect. F: Struct. Biol. Cryst. Commun.* **2006**, *62* (11), 1058−1060.

https://doi.org/10.1021/acsomega.4c05852
ACS Omega 2024, 9, 40034−40050

(23) Mercade, A.; Perez-Enciso, M.; Varona, L.; Alves, E.; Noguera, J. L.; Sanchez, A.; Folch, J. M. Adipocyte fatty-acid binding protein is closely associated to the porcine FAT1 locus on chromosome 4. *J. Anim. Sci.* **2006**, *84* (11), 2907−2913.
(24) Considine, R. V. Human leptin: an adipocyte hormone with weight-regulatory and endocrine functions. *Semin Vasc Med.* **2005**, *5* (01), 15−24.
(25) van Harmelen, V.; Ryden, M.; Sjolin, E.; Hoffstedt, J. A role of lipin in human obesity and insulin resistance: relation to adipocyte glucose transport and GLUT4 expression. *J. Lipid Res.* **2007**, *48* (1), 201−206.
(26) Greenberg, A. S.; Egan, J. J.; Wek, S. A.; Garty, N. B.; Blanchette-Mackie, E. J.; Londos, C. Perilipin, a major hormonally regulated adipocyte-specific phosphoprotein associated with the periphery of lipid storage droplets. *J. Biol. Chem.* **1991**, *266* (17), 11341−11346.
(27) North, R. A. Molecular physiology of P2X receptors. *Physiol Rev.* **2002**, *82* (4), 1013−1067.
(28) Taylor, S. R.; Alexander, D. R.; Cooper, J. C.; Higgins, C. F.; Elliott, J. I. Regulatory T Cells Are Resistant to Apoptosis via TCR but Not P2X7. *J. Immunol.* **2007**, *178* (6), 3474−3482.
(29) Madec, S.; Rossi, C.; Chiarugi, M.; Santini, E.; Salvati, A.; Ferrannini, E.; Solini, A. Adipocyte P2 × 7 receptors expression: a role in modulating inflammatory response in subjects with metabolic syndrome? *Atherosclerosis* **2011**, *219* (2), 552−558.
(30) Morales, L. D.; Cromack, D. T.; Tripathy, D.; Fourcaudot, M.; Kumar, S.; Curran, J. E.; Carless, M.; Goring, H. H. H.; Hu, S. L.; Lopez-Alvarenga, J. C.; Garske, K. M.; Pajukanta, P.; Small, K. S.; Glastonbury, C. A.; Das, S. K.; Langefeld, C.; Hanson, R. L.; Hsueh, W. C.; Norton, L.; Arya, R.; Mummidi, S.; Blangero, J.; DeFronzo, R. A.; Duggirala, R.; Jenkinson, C. P. Further evidence supporting a potential role for ADH1B in obesity. *Sci. Rep.* **2021**, *11* (1), 1932.
(31) Tews, D.; Schwar, V.; Scheithauer, M.; Weber, T.; Fromme, T.; Klingenspor, M.; Barth, T. F.; Möller, P.; Holzmann, K.; Debatin, K. M.; Fischer-Posovszky, P.; Wabitsch, M. Comparative gene array analysis of progenitor cells from human paired deep neck and subcutaneous adipose tissue. *Mol. Cell. Endocrinol.* **2014**, *395* (1−2), 41−50.
(32) Yue, L.; Rasouli, N.; Ranganathan, G.; Kern, P. A.; Mazzone, T. Divergent Effects of Peroxisome Proliferator-activated Receptor γ Agonists and Tumor Necrosis Factor α on Adipocyte ApoE Expression. *J. Biol. Chem.* **2004**, *279* (46), 47626−47632.
(33) Huang, Z. H.; Reardon, C. A.; Mazzone, T. Endogenous ApoE expression modulates adipocyte triglyceride content and turnover. *Diabetes* **2006**, *55* (12), 3394−3402.
(34) Lasrich, D.; Bartelt, A.; Grewal, T.; Heeren, J. Apolipoprotein E promotes lipid accumulation and differentiation in human adipocytes. *Exp. Cell Res.* **2015**, *337* (1), 94−102.
(35) Li, Y. H.; Liu, L. Apolipoprotein E synthesized by adipocyte and apolipoprotein E carried on lipoproteins modulate adipocyte triglyceride content. *Lipids Health Dis* **2014**, *13*, 136.
(36) Bogner-Strauss, J. G.; Prokesch, A.; Sanchez-Cabo, F.; Rieder, D.; Hackl, H.; Duszka, K.; Krogsdam, A.; Di Camillo, B.; Walenta, E.; Klatzer, A.; Lass, A.; Pinent, M.; Wong, W. C.; Eisenhaber, F.; Trajanoski, Z. Reconstruction of gene association network reveals a transmembrane protein required for adipogenesis and targeted by PPARγ. *Cell. Mol. Life Sci.* **2010**, *67* (23), 4049−4064.
(37) Tontonoz, P.; Spiegelman, B. M. Fat and Beyond: The Diverse Biology of PPARγ. *Annu. Rev. Biochem.* **2008**, *77*, 289−312.
(38) Dalen, K. T.; Schoonjans, K.; Ulven, S. M.; Weedon-Fekjaer, M. S.; Bentzen, T. G.; Koutnikova, H.; Auwerx, J.; Nebb, H. I. Adipose Tissue Expression of the Lipid Droplet−Associating Proteins S3-12 and Perilipin Is Controlled by Peroxisome Proliferator−Activated Receptor-γ. *Diabetes* **2004**, *53* (5), 1243−1252.
(39) Wolins, N. E.; Skinner, J. R.; Schoenfish, M. J.; Tzekov, A.; Bensch, K. G.; Bickel, P. E. Adipocyte protein S3−12 coats nascent lipid droplets. *J. Biol. Chem.* **2003**, *278* (39), 37713−37721.
(40) Nimura, S.; Yamaguchi, T.; Ueda, K.; Kadokura, K.; Aiuchi, T.; Kato, R.; Obama, T.; Itabe, H. Olanzapine promotes the accumulation of lipid droplets and the expression of multiple perilipins in human adipocytes. *Biochem. Biophys. Res. Commun.* **2015**, *467* (4), 906−912.
(41) Lu, X.; Gruia-Gray, J.; Copeland, N. G.; Gilbert, D. J.; Jenkins, N. A.; Londos, C.; Kimmel, A. R. The murine perilipin gene: the lipid droplet-associated perilipins derive from tissue-specific, mRNA splice variants and define a gene family of ancient origin. *Mamm. Genome* **2001**, *12* (9), 741−749.
(42) Dichlberger, A.; Schlager, S.; Lappalainen, J.; Kakela, R.; Hattula, K.; Butcher, S. J.; Schneider, W. J.; Kovanen, P. T. Lipid body formation during maturation of human mast cells. *J. Lipid Res.* **2011**, *52* (12), 2198−2208.
(43) Nose, F.; Yamaguchi, T.; Kato, R.; Aiuchi, T.; Obama, T.; Hara, S.; Yamamoto, M.; Itabe, H. Crucial role of perilipin-3 (TIP47) in formation of lipid droplets and PGE2 production in HL-60-derived neutrophils. *PLoS One* **2013**, *8* (8), No. e71542.
(44) Kleinert, M.; Parker, B. L.; Chaudhuri, R.; Fazakerley, D. J.; Serup, A.; Thomas, K. C.; Krycer, J. R.; Sylow, L.; Fritzen, A. M.; Hoffman, N. J.; Jeppesen, J.; Schjerling, P.; Ruegg, M. A.; Kiens, B.; James, D. E.; Richter, E. A. mTORC2 and AMPK differentially regulate muscle triglyceride content via Perilipin 3. *Mol. Metab* **2016**, *5* (8), 646−655.
(45) Grevengoed, T. J.; Klett, E. L.; Coleman, R. A. Acyl-CoA metabolism and partitioning. *Annu. Rev. Nutr.* **2014**, *34*, 1−30.
(46) Kassan, A.; Herms, A.; Fernandez-Vidal, A.; Bosch, M.; Schieber, N. L.; Reddy, B. J.; Fajardo, A.; Gelabert-Baldrich, M.; Tebar, F.; Enrich, C.; Gross, S. P.; Parton, R. G.; Pol, A. Acyl-CoA synthetase 3 promotes lipid droplet biogenesis in ER microdomains. *J. Cell Biol.* **2013**, *203* (6), 985−1001.
(47) Fujimoto, Y.; Itabe, H.; Kinoshita, T.; Homma, K. J.; Onoduka, J.; Mori, M.; Yamaguchi, S.; Makita, M.; Higashi, Y.; Yamashita, A.; Takano, T. Involvement of ACSL in local synthesis of neutral lipids in cytoplasmic lipid droplets in human hepatocyte HuH7. *J. Lipid Res.* **2007**, *48* (6), 1280−1292.
(48) Gerhold, D. L.; Liu, F.; Jiang, G.; Li, Z.; Xu, J.; Lu, M.; Sachs, J. R.; Bagchi, A.; Fridman, A.; Holder, D. J.; Doebber, T. W.; Berger, J.; Elbrecht, A.; Moller, D. E.; Zhang, B. B. Gene expression profile of adipocyte differentiation and its regulation by peroxisome proliferator-activated receptor-gamma agonists. *Endocrinology* **2002**, *143* (6), 2106−2118.
(49) Durgan, D. J.; Smith, J. K.; Hotze, M. A.; Egbejimi, O.; Cuthbert, K. D.; Zaha, V. G.; Dyck, J. R.; Abel, E. D.; Young, M. E. Distinct transcriptional regulation of long-chain acyl-CoA synthetase isoforms and cytosolic thioesterase 1 in the rodent heart by fatty acids and insulin. *Am. J. Physiol.: Heart Circ. Physiol.* **2006**, *290* (6), H2480−H2497.
(50) Rossi Sebastiano, M.; Konstantinidou, G. Targeting Long Chain Acyl-CoA Synthetases for Cancer Therapy. *Int. J. Mol. Sci.* **2019**, *20* (15), 3624.
(51) Daikoku, T.; Shinohara, Y.; Shima, A.; Yamazaki, N.; Terada, H. Dramatic enhancement of the specific expression of the heart-type fatty acid binding protein in rat brown adipose tissue by cold exposure. *FEBS Lett.* **1997**, *410* (2−3), 383−386.
(52) Vergnes, L.; Chin, R.; Young, S. G.; Reue, K. Heart-type fatty acid-binding protein is essential for efficient brown adipose tissue fatty acid oxidation and cold tolerance. *J. Biol. Chem.* **2011**, *286* (1), 380−390.
(53) Yamamoto, T.; Yamamoto, A.; Watanabe, M.; Kataoka, M.; Terada, H.; Shinohara, Y. Quantitative evaluation of the effects of cold exposure of rats on the expression levels of ten FABP isoforms in brown adipose tissue. *Biotechnol. Lett.* **2011**, *33* (2), 237−242.
(54) Jehl-Pietri, C.; Bastie, C.; Gillot, I.; Luquet, S.; Grimaldi, P. A. Peroxisome-proliferator-activated receptor delta mediates the effects of long-chain fatty acids on post-confluent cell proliferation. *Biochem. J.* **2000**, *350* (1), 93−98.
(55) Klebanoff, S. J. Myeloperoxidase-halide-hydrogen peroxide antibacterial system. *J. Bacteriol.* **1968**, *95* (6), 2131−2138.
(56) Coelho, D.; Kim, J. C.; Miousse, I. R.; Fung, S.; du Moulin, M.; Buers, I.; Suormala, T.; Burda, P.; Frapolli, M.; Stucki, M.; Nurnberg,

https://doi.org/10.1021/acsomega.4c05852
ACS Omega 2024, 9, 40034−40050

P.; Thiele, H.; Robenek, H.; Hohne, W.; Longo, N.; Pasquali, M.; Mengel, E.; Watkins, D.; Shoubridge, E. A.; Majewski, J.; Rosenblatt, D. S.; Fowler, B.; Rutsch, F.; Baumgartner, M. R. Mutations in ABCD4 cause a new inborn error of vitamin B12 metabolism. *Nat. Genet.* **2012**, *44* (10), 1152−1155.
(57) Lettieri Barbato, D.; Tatulli, G.; Aquilano, K.; Ciriolo, M. R. FoxO1 controls lysosomal acid lipase in adipocytes: implication of lipophagy during nutrient restriction and metformin treatment. *Cell Death Dis.* **2013**, *4* (10), No. e861.
(58) Griffin, M. J. On the Immunometabolic Role of NF-κB in Adipocytes. *Immunometabolism* **2022**, *4* (1), No. e220003.
(59) Martinelli, S.; Krumbach, O. H. F.; Pantaleoni, F.; Coppola, S.; Amin, E.; Pannone, L.; Nouri, K.; Farina, L.; Dvorsky, R.; Lepri, F.; Buchholzer, M.; Konopatzki, R.; Walsh, L.; Payne, K.; Pierpont, M. E.; Vergano, S. S.; Langley, K. G.; Larsen, D.; Farwell, K. D.; Tang, S.; Mroske, C.; Gallotta, I.; Di Schiavi, E.; Della Monica, M.; Lugli, L.; Rossi, C.; Seri, M.; Cocchi, G.; Henderson, L.; Baskin, B.; Alders, M.; Mendoza-Londono, R.; Dupuis, L.; Nickerson, D. A.; Chong, J. X.; Meeks, N.; Brown, K.; Causey, T.; Cho, M. T.; Demuth, S.; Digilio, M. C.; Gelb, B. D.; Bamshad, M. J.; Zenker, M.; Ahmadian, M. R.; Hennekam, R. C.; Tartaglia, M.; Mirzaa, G. M.; Mirzaa, G. M. Functional Dysregulation of CDC42 Causes Diverse Developmental Phenotypes. *Am. J. Hum. Genet.* **2018**, *102* (2), 309−320.
(60) Lees-Miller, J. P.; Heeley, D. H.; Smillie, L. B.; Kay, C. M. Isolation and characterization of an abundant and novel 22-kDa protein (SM22) from chicken gizzard smooth muscle. *J. Biol. Chem.* **1987**, *262* (7), 2988−2993.
(61) Lucero, D.; Dikilitas, O.; Mendelson, M. M.; Aligabi, Z.; Islam, P.; Neufeld, E. B.; Bansal, A. T.; Freeman, L. A.; Vaisman, B.; Tang, J.; Combs, C. A.; Li, Y.; Voros, S.; Kullo, I. J.; Remaley, A. T. Transgelin: a new gene involved in LDL endocytosis identified by a genome-wide CRISPR-Cas9 screen. *J. Lipid Res.* **2022**, *63* (1), 100160.
(62) Elsafadi, M.; Manikandan, M.; Dawud, R. A.; Alajez, N. M.; Hamam, R.; Alfayez, M.; Kassem, M.; Aldahmash, A.; Mahmood, A. Transgelin is a TGFβ-inducible gene that regulates osteoblastic and adipogenic differentiation of human skeletal stem cells through actin cytoskeleston organization. *Cell Death Dis.* **2016**, *7* (8), No. e2321.
(63) Ismail, A. A.; Fahmy, E. I. Pregnancy-specific β1-glycoprotein (SP1) and its relation to fetal birth weight at term pregnancy. *Eur. J. Obstet Gynecol Reprod Biol.* **1992**, *45* (1), 13−17.
(64) Zhou, G. Q.; Baranov, V.; Zimmermann, W.; Grunert, F.; Erhard, B.; Mincheva-Nilsson, L.; Hammarstrom, S.; Thompson, J. Highly specific monoclonal antibody demonstrates that pregnancy-specific glycoprotein (PSG) is limited to syncytiotrophoblast in human early and term placenta. *Placenta* **1997**, *18* (7), 491−501.
(65) Motran, C. C.; Diaz, F. L.; Gruppi, A.; Slavin, D.; Chatton, B.; Bocco, J. L. Human pregnancy-specific glycoprotein 1a (PSG1a) induces alternative activation in human and mouse monocytes and suppresses the accessory cell-dependent T cell proliferation. *J. Leukoc Biol.* **2002**, *72* (3), 512−521.
(66) Maquoi, E.; Demeulemeester, D.; Voros, G.; Collen, D.; Lijnen, H. R. Enhanced nutritionally induced adipose tissue development in mice with stromelysin-1 gene inactivation. *Thromb. Haemostasis* **2003**, *89* (04), 696−704.
(67) Maquoi, E.; Munaut, C.; Colige, A.; Collen, D.; Lijnen, H. R. Modulation of adipose tissue expression of murine matrix metalloproteinases and their tissue inhibitors with obesity. *Diabetes* **2002**, *51* (4), 1093−1101.
(68) Tsuji, T.; Kelly, N. J.; Takahashi, S.; Leme, A. S.; McGarry Houghton, A.; Shapiro, S. D. Macrophage elastase suppresses white adipose tissue expansion with cigarette smoking. *Am. J. Respir. Cell Mol. Biol.* **2014**, *51* (6), 822−829.
(69) Klaavuniemi, T.; Alho, N.; Hotulainen, P.; Kelloniemi, A.; Havukainen, H.; Permi, P.; Mattila, S.; Ylanne, J. Characterization of the interaction between Actinin-Associated LIM Protein (ALP) and the rod domain of α-actinin. *BMC Cell Biol.* **2009**, *10*, 22.
(70) Kadrmas, J. L.; Beckerle, M. C. The LIM domain: from the cytoskeleton to the nucleus. *Nat. Rev. Mol. Cell Biol.* **2004**, *5* (11), 920−931.
(71) Huang, Z.; Zhou, J. K.; Wang, K.; Chen, H.; Qin, S.; Liu, J.; Luo, M.; Chen, Y.; Jiang, J.; Zhou, L.; Zhu, L.; He, J.; Li, J.; Pu, W.; Gong, Y.; Li, J.; Ye, Q.; Dong, D.; Hu, H.; Zhou, Z.; Dai, L.; Huang, C.; Wei, X.; Peng, Y. PDLIM1 Inhibits Tumor Metastasis Through Activating Hippo Signaling in Hepatocellular Carcinoma. *Hepatology* **2020**, *71* (5), 1643−1659.
(72) Louis, H. A.; Pino, J. D.; Schmeichel, K. L.; Pomies, P.; Beckerle, M. C. Comparison of three members of the cysteine-rich protein family reveals functional conservation and divergent patterns of gene expression. *J. Biol. Chem.* **1997**, *272* (43), 27484−27491.
(73) Miyasaka, K. Y.; Kida, Y. S.; Sato, T.; Minami, M.; Ogura, T. Csrp1 regulates dynamic cell movements of the mesendoderm and cardiac mesoderm through interactions with Dishevelled and Diversin. *Proc. Natl. Acad. Sci. U.S.A.* **2007**, *104* (27), 11274−11279.
(74) Hoffmann, C.; Mao, X.; Dieterle, M.; Moreau, F.; Al Absi, A.; Steinmetz, A.; Oudin, A.; Berchem, G.; Janji, B.; Thomas, C. CRP2, a new invadopodia actin bundling factor critically promotes breast cancer cell invasion and metastasis. *Oncotarget* **2016**, *7* (12), 13688−13705.
(75) Nystrom, A.; Bruckner-Tuderman, L. Matrix molecules and skin biology. *Semin. Cell Dev. Biol.* **2019**, *89*, 136−146.
(76) Jaaskelainen, I.; Petaisto, T.; Mirzarazi Dahagi, E.; Mahmoodi, M.; Pihlajaniemi, T.; Kaartinen, M. T.; Heljasvaara, R. Collagens Regulating Adipose Tissue Formation and Functions. *Biomedicines* **2023**, *11* (5), 1412.
(77) Mauney, J. R.; Nguyen, T.; Gillen, K.; Kirker-Head, C.; Gimble, J. M.; Kaplan, D. L. Engineering adipose-like tissue in vitro and in vivo utilizing human bone marrow and adipose-derived mesenchymal stem cells with silk fibroin 3D scaffolds. *Biomaterials* **2007**, *28* (35), 5280−5290.
(78) Taura, D.; Noguchi, M.; Sone, M.; Hosoda, K.; Mori, E.; Okada, Y.; Takahashi, K.; Homma, K.; Oyamada, N.; Inuzuka, M.; Sonoyama, T.; Ebihara, K.; Tamura, N.; Itoh, H.; Suemori, H.; Nakatsuji, N.; Okano, H.; Yamanaka, S.; Nakao, K. Adipogenic differentiation of human induced pluripotent stem cells: comparison with that of human embryonic stem cells. *FEBS Lett.* **2009**, *583* (6), 1029−1033.
(79) Ahfeldt, T.; Schinzel, R. T.; Lee, Y. K.; Hendrickson, D.; Kaplan, A.; Lum, D. H.; Camahort, R.; Xia, F.; Shay, J.; Rhee, E. P.; Clish, C. B.; Deo, R. C.; Shen, T.; Lau, F. H.; Cowley, A.; Mowrer, G.; Al-Siddiqi, H.; Nahrendorf, M.; Musunuru, K.; Gerszten, R. E.; Rinn, J. L.; Cowan, C. A. Programming human pluripotent stem cells into white and brown adipocytes. *Nat. Cell Biol.* **2012**, *14* (2), 209−219.
(80) Choi, S.; Goswami, N.; Schmidt, F. Comparative Proteomic Profiling of 3T3-L1 Adipocyte Differentiation Using SILAC Quantification. *J. Proteome Res.* **2020**, *19* (12), 4884−4900.
(81) Siersbaek, R.; Mandrup, S. Transcriptional networks controlling adipocyte differentiation. *Cold Spring Harbor Symp. Quant. Biol.* **2011**, *76*, 247−255.
(82) Farmer, S. R. Transcriptional control of adipocyte formation. *Cell Metab.* **2006**, *4* (4), 263−273.
(83) Yehuda-Shnaidman, E.; Buehrer, B.; Pi, J.; Kumar, N.; Collins, S. Acute stimulation of white adipocyte respiration by PKA-induced lipolysis. *Diabetes* **2010**, *59* (10), 2474−2483.
(84) Lee, Y. S.; Kim, J. W.; Osborne, O.; Oh, D. Y.; Sasik, R.; Schenk, S.; Chen, A.; Chung, H.; Murphy, A.; Watkins, S. M.; Quehenberger, O.; Johnson, R. S.; Olefsky, J. M. Increased Adipocyte O2 Consumption Triggers HIF-1α, Causing Inflammation and Insulin Resistance in Obesity. *Cell* **2014**, *157* (6), 1339−1352.
(85) Su, Q. Q.; Tian, Y. Y.; Liu, Z. N.; Ci, L. L.; Lv, X. W. Purinergic P2X7 receptor blockade mitigates alcohol-induced steatohepatitis and intestinal injury by regulating MEK1/2-ERK1/2 signaling and egr-1 activity. *Int. Immunopharmacol.* **2019**, *66*, 52−61.
(86) Beaucage, K. L.; Xiao, A.; Pollmann, S. I.; Grol, M. W.; Beach, R. J.; Holdsworth, D. W.; Sims, S. M.; Darling, M. R.; Dixon, S. J. Loss of P2X7 nucleotide receptor function leads to abnormal fat distribution in mice. *Purinergic Signalling* **2014**, *10* (2), 291−304.

https://doi.org/10.1021/acsomega.4c05852
ACS Omega 2024, 9, 40034−40050

(87) Li, J.; Gong, L.; Xu, Q. Purinergic 2X7 receptor is involved in adipogenesis and lipid degradation. *Exp. Ther. Med.* **2022**, *23* (1), 81.
(88) Gao, H.; Li, D.; Yang, P.; Zhao, L.; Wei, L.; Chen, Y.; Ruan, X. Z. Suppression of CD36 attenuates adipogenesis with a reduction of P2X7 expression in 3T3-L1 cells. *Biochem. Biophys. Res. Commun.* **2017**, *491* (1), 204−208.
(89) Welsh, G. I.; Griffiths, M. R.; Webster, K. J.; Page, M. J.; Tavare, J. M. Proteome analysis of adipogenesis. *Proteomics* **2004**, *4* (4), 1042−1051.
(90) Frühbeck, G.; Catalán, V.; Rodríguez, A.; Gómez-Ambrosi, J. Adiponectin-leptin ratio: A promising index to estimate adipose tissue dysfunction. Relation with obesity-associated cardiometabolic risk. *Adipocyte* **2018**, *7* (1), 57−62.

https://doi.org/10.1021/acsomega.4c05852
ACS Omega 2024, 9, 40034−40050